UNIVERSITAT DE BARCELONA

Final Degree Project

Biomedical Engineering Degree

Study of systems powered by triboelectric generators for bioengineering applications

Barcelona, 14 of June of 2021

Author: Helena Rodríguez González

Director: Pere Lluís Miribel Català | Co-director: Manel Puig i Vidal

Acknowledgement

I would like to express my sincere thanks to Pere Lluís Miribel and Manel Puig, for their time, interest and guidance that have helped me to conceive and develop this project.

This Final Degree project has been carried out in the frame of the project *Plataformas Sensoras Inteligentes Auto-Alimentadas para la industria 4.0*, PID2019-110142RB-C22/AEI/10.13039/501100011033

Abstract

The finite lifespan of batteries in implants and wearables generates the necessity to look for energy harvesting methods to avoid having to replace the power supply of different medical devices. This project focuses on the study of triboelectric nanogenerators (TENGs) as a power source for devices applied to bioengineering.

These generators are based on the appearance of a potential difference from the accumulation of charges on two parallel surfaces due to electrostatic electricity. Understanding the physics of the voltage source enables us to generate an electric model of the TENG. When simulating, an oscillating DC electric output is obtained, with a maximum open circuit voltage of 1.8kV, which varies depending on the material parameters. Power management circuits are needed in order to obtain a stable DC voltage from the irregular AC tension. It has been studied the performance of an AC/DC rectifier bridge, which has shown to provide a stable DC output signal but low efficiency (~66.2%).

Furthermore, an ultra-simple TENG (U-TENG) has been manufactured [1] (Mallineni et al., 2017) and it has been demonstrated the triboelectric effect, as voltage appears when applying a periodic force to change separation between plates. However, the maximum open circuit voltage obtained is much lower compared with the ones described in the article, 5.3 V compared to 480 V. Dependence on surface has also been demonstrated.

Finally, when comparing the electric output of TENGs with the supply requirements of some important implantable medical devices, TENGs have demonstrated to be a suitable solution for self-feeding systems.

1 INDEX

2 INTRODUCTION

2.1 OBJECTIVES OF THE PROJECT

The main objective of this Final Degree Project is to study triboelectric generators, the U-TENG specifically [1] (Mallineni et al., 2017) and its applications in the field of bioengineering. This technology is still in development, although there are studies that demonstrate the good performance and efficacy of triboelectric generators in the medical field. That is why this project may result of special interest in the area, as it may contribute knowledge in a field that still requires research.

The triboelectric generators are based on systems that allow taking advantage of the potential difference caused by the accumulation of charges due to friction between different materials [2] (Shi, Li, & Fan, 2018). This friction can be obtained from basic biological activities and, thanks to the recovery electronics, an alternating current can be obtained.

The main objective of the development of triboelectric generators is to create devices for harvesting energy from human motion, walking, vibration, mechanical triggering, rotating tire, wind, flowing water, among others [2] (Shi et al., 2018). Furthermore, the electrical signal can be measured and therefore can be a biosensor for measuring biological stimuli, apart from supplying energy to the device. Within the field of medicine, the main goal is the development of self-powered sensors [2] (Shi et al., 2018).

The study aims to broaden knowledge about the structure of triboelectric generators and ways of building it. Moreover, it has as a goal to discuss the different materials that can be used, as well as its working ranges: voltage, power, etc. In order to go deeper, a triboelectric generator will be manufactured, according to S.S.K. Mallineni et al [1] and will be characterized following the article.

Another general objective is to discuss about possible applications of triboelectric generators in the field of biomedical engineering, specifically for POC wearables and implantable devices, considering the values obtained in the simulation and experimentally.

All these objectives considered, it will be necessary to follow a working process that involves knowing the state of technology, or state of the art, and, from this information, work on a model, defined in S.S.K. Mallineni et al [1]. This model will be simulated, in order to study its behaviour and working ranges. Then, taking basis on the model, a U-TENG will be manufactured, and it will be characterized and tested to see if the results resemble that of the model. Finally, the electronics for energy harvesting will be designed in order to go further with the studies.

Specifically, the particular objectives of this study are:

1. To simulate an electric model of the triboelectric generator, based on previous studies.
2. To study and simulate the performance of different accommodation circuits.
3. To fabricate a triboelectric generator, following the instructions of a previous study.
4. To test the created triboelectric generator and see if the results coincide with the ones of the model chosen.
5. To investigate the effects of materials and dimension of the components chosen on its performance.
6. To make the electrical characterization of the manufactured TENG and study its working ranges, voltage levels and energy recovery levels.
7. To demonstrate its performance as a self-feeding system for bioengineering applications.

2.2 SCOPE OF THE PROJECT

As indicated in the objectives, the project is intended to broaden the knowledge about this type of technology, so that the final deliverables include information and conclusions that can be used for subsequent related studies.

Considering that it is a project that follows an experimental development, its deliverables must be products or devices, the production of which is based on existing knowledge obtained from previous research. It is worth mentioning that, as it is a project of academic motivation, the practical experience that is defined in this project may be used in the future by both the same department and others.

The project has been developed in the Department of Electronic and Biomedical Engineering, in the Faculty of Physics of the University of Barcelona. In addition, it is a project that must be dimensioned for a total time of 300 hours, which is why, despite being a topic that allows a lot of research lines, the project should be reduced and adjusted to spatial and temporal limitations.

	TABLE 1: PROJECT LIMITATIONS	
	INCLUDED	EXCLUDED
ESSENTIAL	Simulation of an electrical model of the triboelectric generator. Manufacturing the triboelectric generator following a model. Use off-the-shelf materials. Obtain data of output values from a simulation of the body activity. Make the electrical characterization of the system. Simulate a Power Management system.	Design a new electrical model for the generator. Implement and design a new type of triboelectric generator. Use materials created with micro/nanopatterning specially made to suit our particular purpose. Use as an input stimulus real human activity.
DESIRABLE	Design the electronics into which integrate the triboelectric generator for a given bioengineering application. To confirm its usefulness specifically for the application chosen. To compare the performance, sensitivity and characteristics of triboelectric generator devices with other strategies commercially available.	Integrate the triboelectric generator into a medical implant or wearable. Fabrication of different types of triboelectric generators to contrast their performance.

Table 1: Project limitations.

Bearing in mind the specific objectives mentioned, we can define the deliverables of the project. The first of these is a simulation and a behavioural study report of the electric model of the triboelectric source, based on de model described in previous studies and already characterized. This study must report power and current-tension values, among other parameters.

Moreover, a manufactured U-TENG of the triboelectric generator is one deliverable to consider, which must meet the conditions defined in the S.S.K. Mallineni et al [1], a commercial and simple to reproduce model. The U-TENG must be accompanied by a document that describes its technical information and its components. The criterion that will make this deliverable product acceptable is the matching of the triboelectric generator created with the materials and structure defined by the model, as well as obtaining an electrical signal from the friction of its components due to an external periodic force.

In addition, another deliverable will be a report that includes the data collected when testing the performance of our triboelectric generator and its electric characterization. The requirements of this report include data on working ranges in voltage and power, as well as information on the output values based on the inputs. In this case, we will consider that it is an acceptable report if it demonstrates the correct performance of the triboelectric generator, based on demonstrating the obtaining of an output signal from a certain stimulus, and the dependence of the output signal on the frequency of the pushing force and dimensions of the triboelectric generator.

Finally, there are some desirable tasks that, if done, would provide to our project more knowledge to understand the applications of triboelectric generators as energy harvesters. Among them, we find the design of the adaptation electronics in a certain application, together with a document that includes data collected after the simulation of human activity and a comparison of its performance with respect to other energy harvesting strategies.

One of the main risks is that, even though there are numerous articles on triboelectric generators and their design, it is worth mentioning that this is an emerging technology and, consequently, the previous research studies on the subject will not be as many as if it were a fully implanted technology.

3 BACKGROUND

3.1 STATE OF ART

3.1.1 Triboelectric generators

In the current technological framework, most medical devices, such as sensors, need an external power source, so that they cannot work independently and sustainably, a factor that has become one of the main restrictions for the development of technology in the medical field. This becomes a problem when talking about implantable biomedical devices, as when their batteries die, they need for surgical interventions to replace them.

To address this problem, it is being studied the combination of these devices with the technology known as energy harvesting. In this way, the generation of self-powered systems is allowed, so that the use of power components such as batteries is avoided, and there is no need for periodical replacement.

The concept of energy harvesting refers to the generation of electrical signals by the same device when detecting stimuli or analytes, such as body movement, touch, pressure, acoustic sound or others [2] (Shi et al., 2018). These systems that obtain electricity from different energy sources are based on principles such as spontaneous redox reactions, the thermoelectric effect, the piezoelectric effect or the triboelectric effect. In our study we will focus on the last one, triboelectric nanogenerators, which are based on mechanical energy.

Triboelectric nanogenerators (TENGs) are based on the triboelectrification principle, which states that an electric charge is generated on the surface of two materials when being fractioned one against the other [3] (Wang, Yang, & Wang, 2017). When the two materials separate from each other, it will behave like a parallel plate capacitor, and a current transfer will take place, by using an external circuit. The electric energy generated will be collected and stored, in order to be used to power the device itself. This energy will depend on the electronegativity of the electrodes, and on the contact area between the electrodes $(U = QV/2)$, so that the materials chosen for the electrodes and matrix will play a crucial role for the sensibility of the TENG.

This technology does not only allow working without external energy sources, but it can also be used for the detection and monitoring of biological processes that involve the release of random mechanical energy. A biological signal is transformed into an electric signal, so if we know the relationship between the biological signal and the output voltage generated by the triboelectric, we can measure voltage and obtain the biological magnitude, what means that triboelectric nanogenerators can work simultaneously as sensors and generators.

As we have already mentioned, it is an existing technology the integration of which results of special interest in the field of bioengineering. Due to its great potential in the field of medical care, robotics, prosthetics and sports, lines of research have been developed in recent years, with the main aim of manufacturing smaller devices with biocompatible materials and high accuracy. These research studies take place specially in universities, engineering colleges and research institutes. It is not a fully implemented technology, even though there are already numerous studies that demonstrate its performance, and therefore it is being investigated with the aim of integrating it into the field of bioengineering. Among the studies carried out, different applications have been discussed, with their corresponding materials and working ranges.

3.1.2 Bioengineering applications

Triboelectric generators are a promising option as energy harvesters, since their ability to generate electrical energy from motion could solve the challenge of the limited lifetime of any energy storage units. The fact that TENGs are effective mechanical to electric converters not only provides the opportunity to use them to create self-powered devices, but also for sensing applications. The energy harvested can be stored in an energy storage unit, for feeding the system, but from this energy information can also be obtained with sensors.

Several fields of application of TENGs have been investigated, including self-powered implantable and wearable systems. Most of them use triboelectric systems as sensors for monitoring different motion parameters, measuring stimuli such as vibrations, body motion, pressure, flow or inclination angles.

Wearable devices are systems can be placed on the human body itself or on clothing and, therefore, are intended to be portable. However, its battery life is one of the main limitations that affects the comfort of its use. Activities such as walking, running or other human motion produce mechanical energy, that can be converted into electrical energy and serve as a power source for these wearable devices.

In the case of implantable devices, the replacement of power supply systems is even more complex, since it requires a surgical intervention. For this reason, it is of special interest to take advantage of the potential creation in a triboelectric generator caused by the movement of the body, such as variations in pressure, vibrations or others.

Recently, an effort on harvesting heartbeat energy is being made for the power supply of pacemakers and in vivo performance in animals is being demonstrated [4] (Z. Wu, Cheng, & Wang, 2020). In Figure 1a, the first in vivo biomechanical harvesting work is observed. Moreover, this TENGs can be developed for continuous monitoring of pathological and physiological signs in the heart rate or breathing (Figure 1b). Other works have been carried out to study in-vivo viability of TENGs, such as searching for biodegradable and resorbable materials (Figure 1c). The output values for this TENG were a maximum open-circuit voltage of 40V and a short circuit current of 1mA. Other examples of implantable TENGs are shown in Figures 1d, 1e and 1f.

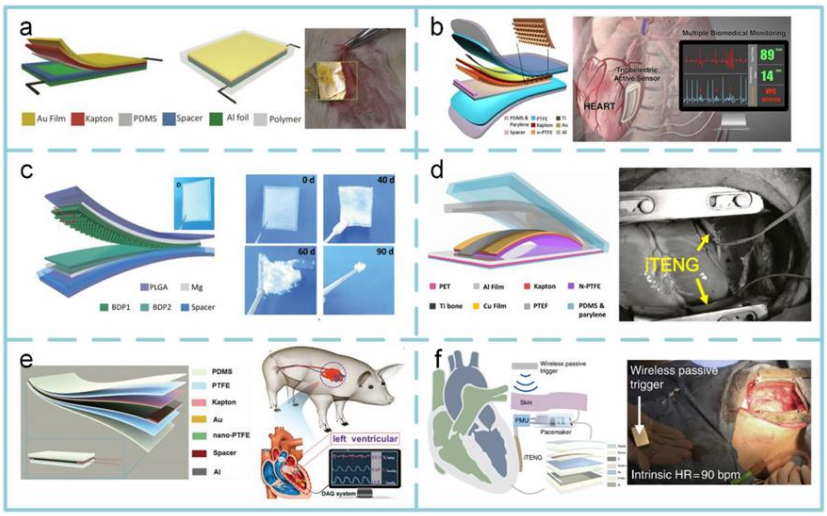

Figure 1: Examples of TENGs applications for implantable biomedical devices. Image from 'Self-Powered Sensors and Systems Based on Nanogenerators' [4] (Z. Wu et al., 2020).

Applications in the biomedical field are not limited only to implantable or wearable devices but also to other types of smart applications [4] (Z. Wu et al., 2020). An example is the application of the triboelectric fluidic sensor used for an infusion monitor (Figure 2a). In addition, thanks to their flexibility, they can also be included in textiles and clothing. This fact allows them to be included in mattresses, to detect the movement of a patient in the bed, and allow sleep monitoring (Figure 2b and 2c). Other smart applications are heart-rate monitoring (figure 2d) and transdermal drug delivery with feedback control (figure 2e and 2f).

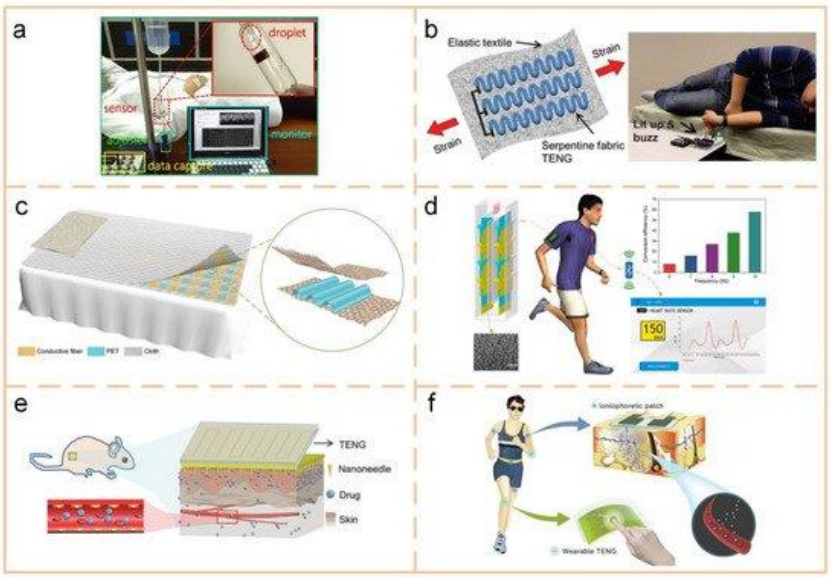

Figure 2: Examples of smart applications of TENGs. Image from 'Self-Powered Sensors and Systems Based on Nanogenerators' [4] (Z. Wu et al., 2020).

Self-powered skin sensors are another potential application [5] (Rao et al., 2019). In Rao et al. classify between those that obtain the mechanical energy of body movement, touch or pressure and acoustic sound. The former, which take advantage of body motion, can monitor the movement and activity of the individual, as well as the movement of joints if placed on them, or even monitor breathing if placed on the chest. Its application was also defined in the detection of pressures produced in the body, such as voice, blood pressure, heartbeat or respiratory movement, as well as for acoustic sound, which results of special interest in the development of hearing aids.

Chuan et al. [6] reported another example are the rotational speed sensors for turbodrills. These ones make use of the TENG to measure the rotational speed of the turbodrill in real time and self-powering. It has been demonstrated that the energy that is generated supplies the power requirements of the sensor and could power other instruments.

TENGs application in gas flowmeters was also discussed by Trung et al. [7]. Its structure is based on a circular pipe in which a thin non-conductive membrane is located between two copper electrodes. When gas flows inside the pipe, the membrane oscillates between the two electrodes and periodic electrical potential is generated, the frequency of which is proportional to the flow rate. Among the advantages of making use of triboelectric generators for flowmeters, against the typical types, such as ultrasonic, coriolis and vortex ones, we find a high sensitivity of the measured flow, a lower pressure loss, apart from the fact that the generated voltage can also be used for self-feeding the device.

Apart from the mentioned applications, there have been carried out studies that provide evidence on the performance and effectiveness of other types of applications, as well as researches on potential future

applications [8, 9, 10, 11] (Chen et al., 2019)(Vibration, 2020)(Lee, Lee, & Baik, 2018)(C. Wu, Wang, Ding, Guo, & Wang, 2019).

3.1.3 U-TENG

It is important to have a vision of what are the voltage levels, currents involved, and the energy generated in order to determine what their potential applications will be. In S.S.K. Mallineni et. al. [1], it is detailed the construction process of the ultra-simple triboelectric nanogenerator (U-TENG) and the energy levels and working ranges that are achieved according to size and frequency of work.

The U-TENG is formed by plates made of PET coated with ITO, a commercially available material that consist on a polymer covered with a liquid conductive layer, that works as the two electrodes. A layer of Kapton is attached to the lower electrode, and behaves as the triboelectric layer. Both electrodes are kept separated by Pyrex insulating spacers. U-TENGs are, therefore, easy to build and low-cost.

The electrical characterization of the U-TENG, with dimensions 3.5 cm × 2.75 cm, was performed by applying a periodic vertical force of ~ 50 N, at low frequencies (2 Hz), dropped from a height of 1 cm, which corresponds to a potential energy of 0.5 J. In order to apply this periodic force, a motorized pushing tester was manually built. Under these conditions, the U-TENG exhibited a maximum open-circuit output voltage (VOC) of ~ 120 V, a voltage value much lower than that predicted by theoretical MSCD-based COMSOL simulations (~ 4000 V).

In order to increase the loads and, consequently, the output voltage, a cellulose paper, which is highly electropositive, was inserted between the ITO and Kapton electrodes. Only by inserting the cellulose paper was it possible to increase the Voc to ~ 480 V. The other parameters measured were a short-circuit current (ISC) of ~ 50 μA, and maximum peak power of 1.7 mW. The power density values obtained were ~ 190 μW cm −2, considering the total area of the device, and ~ 490 μW cm −2, considering only the area of contact with the pushing tester (diameter ~ 20 mm).

Finally, it is worth mentioning that by increasing the frequency with which the mechanical force is applied (> 10 Hz) higher charge densities can be achieved. Also, the U-TENGs support a wide range of load conditions, around 1–160 MΩ, without a significant loss in the output and there is no performance loss with fatigue (for more than 20,000 cycles).

3.2 PROJECT ENVIRONMENT

This project is created with the intention of continuing studies that have been previously developed on triboelectric nanogenerators in the area of biomedical engineering, and to provide information on their performance, and bases for subsequent studies.

Biomedical engineering is a field that is in continuous growth and development globally. In Spain there are more than a thousand companies that are economically involved in biotech areas. To this, research units from hospitals and universities, and research centres are added. Furthermore, the biomedical engineering academic community and industry is supported by the SEIB (*Sociedad Española de Ingeniería Biomédica*). It is composed by more than 30 research groups in the different areas of biomedical engineering, such as the BSICOS Group, ISI or CEIT. SEIB is affiliated with the International Federation for Medical and Biological Engineering (IFMBE) and the European Alliance for Medical and Biological Engineering and Science (EAMBES).

If we refer to the regulation framework, since the project does not intend to design a triboelectric generator to be subsequently integrated into an implant or wearable for medical use, it is not necessary that they meet the requirements set forth by the respective rules and regulations. Even so, the one fabricated in this project will work with biocompatible materials to contextualize it in the field of medical devices. If it was intended to integrate it into a medical device and commercialize, it would be necessary to be under the regulations and standards, which are stricter in the case of life support devices.

In addition, it is also within environmental regulations, since these systems are based on the generation of sustainable and renewable energy, which is obtained from human body activity, and avoids the use of batteries or other less clean energy sources.

It is worth to bear in mind that it is an emerging technology that can be manufactured through innovative nanomaterials and polymers, such as graphene and carbon nanotubes, PDMS or others. Therefore, the development of our technology will depend on the evolution of the materials market and the appearance of new materials. In addition, our market will also evolve according to demand, so that the more bioengineering companies are interested in our technology, the more investment there will be for its development. It should be said that it is a market that is highly dependent on private financing.

4 MARKET ANALYSIS

Research on triboelectric nanogenerators, as we have already mentioned, is a booming sector. R&D area of companies, research centres, universities and hospitals are working on the development and improvement of this technology.

Not only do those who develop TENGs work on energy harvesting, but they share their goals with other types of self-feeding systems based on other types of energies, such as those based on piezoelectric effect, biofuel cells, endocochlear potential, light or body temperature [12] (Fan, Tian, & Lin Wang, 2012).

An example of alternative systems based on energy harvesting are self-powered biofuel cells, for example those that take advantage of the energy generated in metabolic processes by enzymes. It is a technology with great potential, but it has limitations such as short lifetimes and reduced performance resulting from slow direct electron transfer. Furthermore, temperature alters the activity and stability of enzymes.

One of main substitute technologies is the use of piezoelectric nanogenerators (PENGs), that also obtain electricity from mechanical energy. Unlike triboelectric nanogenerators, PENGs can only make use of limited types of materials, piezoelectric materials, therefore allowing little margin for variation. Because of this reason, the cost of piezoelectric devices may be expensive, as micromachining sophisticated technologies are required. Furthermore, those materials with a higher piezoelectric coefficient are less flexible, a necessary feature in some implantable devices.

Moreover, we can find hybrid energy harvesting methods based on coupling different fields. For instance, we may find a combination of a triboelectric with a piezoelectric, with a photovoltaic or with a electrochemical method.

The benefits of TENGs devices, with respect to its substitutive products, are their simple manufacturing and simple structure, as well as the low cost of the process of fabrication and materials. The main advantage over piezoelectric based devices is that TENGs can use a wide variety of materials for their components. Among the most frequently used materials we find rubber or silicone elastomers, coated textiles and flexible films, which often are fabricated with 3D printing.

The portfolio of potential clients is highly diversified, given the wide usefulness of this technology in various types of medical devices. The main target sectors are companies for medical diagnostic, monitoring and therapy equipment; as well as any other company dedicated to medical technology, specifically mechanical sensors or implantable or wearable systems that require self-feeding.

4.1 HISTORICAL EVOLUTION AND FUTURE PROSPECTS OF THE MARKET

The physical phenomenon on which this type of generators is based, the triboelectric effect, has been known for centuries. As early as the 17th century, Francis Hauksbee manufactured a triboelectric electrostatic generator [11] (C. Wu et al., 2019), based on Otto von Guericke's electrostatic generator. Despite being a known and described physic principle, the first flexible triboelectric nanogenerator was invented in 2012, by Prof. Zhong Lin Wang's group [12] (Fan et al., 2012).. In 2006, this same group had developed the first piezoelectric nanogenerator, from ZnO nanowires.

The innovation introduced by Zhong Lin Wang's team from the Georgia Tech Institute was the proposal to make use of triboelectric nanogenerators as mechanical energy harvesters. Since then, research has focused on exploring its applications and its commercialization potential, but the main challenge to overcome has been that the power output was very low.

With the aim of improving efficiency and power output, several studies have been carried out [13] (Zhong Lin Wang et al., 2015), demonstrating and reaching values for output area power density of 500 W m^{-2} and total energy conversion efficiency of up to 85% [2] (Shi et al., 2018).

In 2017, the ultra-simple triboelectric nanogenerator (U-TENG) was invented by a group of physicists at the Clemson Nanomaterials Institute, S.S.K. Mallineni et al. [1], which is the one that will be taken as a model for this project. Under this same premise, the W-TENG was designed, which used materials of such opposite affinities that they generated enough electric field to be used for wireless connections.

This technology opens doors to generate renewable energy from clean sources, including the one produced by the daily movement of the human body. As we have mentioned, the research lines seek to improve performance and power density, so that in the future it is intended to obtain devices capable of charging batteries from smartwatches or phones.

But, so far, one of the limitations of the projects still being the maximum level of energy transformed by the device at its maximum performance. Therefore, it results interesting for enterprises and investigation institutes to work on initiatives based on the design of a device that can potentially supply the needs of the energetic market.

Currently, triboelectric generators are already in development stage, as their use as energy harvesting devices is new. Despite it has been demonstrated its good performance, there are still being needed more studies to make it a competitive system in the market. Therefore, inversion costs in the development of these devices may not be very high, but neither will be the benefits, at least in a short period of time. With research and evolution in this technology, it may become a potential option for energy generation.

The power levels at which the triboelectric generators work determine the applications that can be applied to them. So far, the triboelectric generator, due to its robustness and biocompatibility characteristics, has been shown to be intended to work for implantable devices.

Speaking of the market projection, we can say that it is a growing market of constant demand. Since it shows great potential for growth and development, as well as proliferation and integration in the medical field. Furthermore, given their simple structure and manufacturing process, the cost of these devices is low, which makes triboelectric nanogenerators a sustainable and economical alternative to current power supplies.

5 CONCEPTION ENGINEERING

This chapter aims, once the state of the art is known, to select the orientation that the project will take, as well as the choice of a model on which to base it.

5.1 PROJECT ORIENTATION

5.1.1 Solution study

The study of triboelectric generators can be approached from different perspectives and orientations, depending on the type of study we want to do and the data to obtain.

One possible orientation of the project is to model a generator element, its design and simulation of the circuit with a simulation software. This can be done with a Spice (Simulation Program with Integrated Circuit Emphasis) type software, which can perform different types of analysis and has a wide variety of elements to simulate the circuit. It is a very powerful and useful tool, if the data is supplied correctly, as it reduces the analysis time. Among the Spice software that are available, LTSpice [14] allows free access from any computer. These types of simulators are based on three procedures: definition of the characteristics of the elements that are part of the circuit, running the program and creation of an output file, and indicating to the program how to present the results obtained.

The Spice model would allow us to know if the designed circuit works or not, how the circuit behaves and to make simulations in time, frequency or others. In this way, the signal generation of the triboelectric generator could be simulated, and numerical calculations could be performed for the analysis of the circuit. Otherwise, despite modelling the generator element with a Spice program allows an exhaustive study on the behaviour of triboelectric generators, the conditioning electronics and the realization of complex mathematical calculations in a short period of time, it is limited to a theoretical study of the ideal operation of triboelectric generators.

With the LTSpice simulation, triboelectric generator output signal, and the characterization of the conditioning circuit that surrounds it can be obtained. However, if we are interested on studying the triboelectric generator structure and the properties of its materials, a possible approach is manufacturing one.

There are several articles on the manufacture of triboelectric generators, in which they discuss the process or methodology that is followed to control it [15] (Rodrigues-marinho, Castro, Correia, Costa, & Lanceros-méndez, 2020). In Rodrigues-Marinho et. al., an evaluation of the power output is made as a function of different pairs of polymers or polymer compounds. The different materials compared occupy different positions in the triboelectric series, but are also distinguished in their dielectric constant and surface roughness.

It has been reported that the output current and voltage depend proportionally on the charge density of the triboelectric surface, in such a way that the power is proportional to the square of charge density [11] (C. Wu et al., 2019). Generally, several studies have been carried out in order to improve the electrical output of triboelectric generators, an objective that can be reached by increasing the charge generation [16] (Kim, Lee, Kim, & Jeong, 2020).

One of the main approaches to be considered for performance enhancement is increasing contact area, by fabricating microscale or nanoscale structures so that the effective surface is increased. Among the proposed methods to fabricate these micropatterns we find soft lithography, nanotubes deposition, force-

assembled colloidal arrays, surface nanomaterial fabrication or others [17] (Lee et al., 2017). It has also been reported that surface charge generation can be improved by increasing the adhesion energy [18] (Hinchet et al., 2018).

Another approach worth mentioning focus on materials and material designs. One of the main strategies is surface functionalization for material modification, such as increasing surface charge density or facilitate charge transfer, and bulk composition manipulation [11] (C. Wu et al., 2019). Ion doping, radical injection and plasma treatment are techniques that may enhance charge generation. Thanks to chemical surface functionalization, the functional groups of the triboelectric layer are exposed on the surface so that charge capture capability is improved. Moreover, output power can be increased thanks to electron-donating and electron-withdrawing functional end groups of the layer surface [16] (Kim et al., 2020).

Intrinsic material properties, such as dielectric constant or polarity, can be changed as a strategy for performance improvement. For example, when polarizing ferroelectric polymers by electric poling, a better triboelectrification is observed. Other techniques for material modification are chemical doping and nanocomposite formation. It is also interesting to delve into the development and creation of new materials through molecular synthesis or the formation of nanocomposites.

However, all these advanced techniques for charge density optimization would suppose an increase of time and cost. Therefore, simple structure, low complexity and wide range of materials determine a low overall cost of the fabrication process of triboelectric generators.

In the case of manufacturing a triboelectric generator, one could try to design a new idea of a triboelectric, or manufacture one based on a model defined in previous studies. The option of designing one from scratch requires a lot of prior knowledge and studies on the subject, which entails more time than the one we have. In addition, there are several studies that explain in detail the manufacturing process of triboelectric generators, which could facilitate the process.

5.1.2 Proposed solution

All these things considered, the option that provides a theoretical and experimental view of triboelectric generators and its performance is to simulate its behaviour in a Spice-type program and to further manufacture one.

Firstly, the TENG will be modelled and simulated. Then, the integration electronics will be designed, for which a Spice-type program can be used to simulate the operation of different accommodation circuits prior to its manufacture.

The option that focuses more on triboelectric generators structure is to manufacture one. The construction will be done through materials that meet conditions of flexibility, reliability and biocompatibility, of which there is natural abundance. Low cost commercially available materials will be used, so that nanopatterning will not be necessary. But this strategy has some risks associated, which will be discussed in the next chapter, that may hinder the development and manufacturing of the product. Once built, the U-TENG will be characterized, and the parameters obtained can be introduced to the LTSpice simulation, in order to adapt it to our model.

In order to facilitate the construction process, a previously defined model will be used on which we will base for the design of our triboelectric generator. That is why we must also define which model we will use for our project.

5.2 MANUFACTURING MODEL

5.2.1 Solution study

A model to consider is the triboelectric defined in 2012 by Fan et al. [12] (Fan et al., 2012). It consists on a two polymer sheets sandwiched structure. The polymers used are a Kapton film placed onto a PET substrate. Bottom and top structures are coated with a thin layer of Au alloy film, that produces two mobile charges, of the same modulus and opposite sign, in the interfacial region. Moreover, the coatings behave as electrodes, that are directly connected to an external circuit. The maximum output voltage obtained was 3.3V and a peak output power density of 10.4 mW/cm^3.

Another possibility is to follow the model described in S.S.K. Mallineni et al [1]. The U-TENG top and bottom electrodes are made of a commercially available material, PET coated with ITO. To the bottom electrode it is also adhered a Kapton film and four Pyrex insulating spacers create an air gap that separates the electrodes. The values obtained from this device were a maximum output voltage of 480V and output power density of ~490 μW cm.

In the study made by Jihong Rao et al. [5], several materials that can be used in the context of skin sensors are described. Among the mentioned materials stretchable materials are one of the most used, such as PDMS or rubbers, with an aluminium foil or gold nanolayers, for which an output power density value of 76.27 W m^{-2} is obtained. In addition, it also refers to the use of textiles covered with a layer of PEDOT: PSS or flexible films, with output power density values of 2 W m^{-2} and 5 W m^{-2}, respectively. However, this article does not explain in as much detail the construction of the triboelectric generator as in the previous two, as it focuses more on applications.

In the other articles found about triboelectric generators, such as the gas flowmeter, by Trung et al. [7], uses of triboelectric generators for self-powering devices are defined, so that they focus more on potential applications and measured values of their performance, than on the explanation of its manufacturing.

5.2.2 Proposed solution

The model on which we will rely for the manufacture of the triboelectric generator is the one defined in the article by Mallineni et al. [1]. This is one of the most detailed articles, both in the explanation of the manufacture and the characterization of the electrical circuit. Moreover, it does not require pre-processing, since commercially available materials are used that do not require micro-patterning or metal-electrode deposition, so it reduces manufacturing costs and time required. Its robustness and easy reproducibility make this article a suitable model on which we can base our project.

As we have mentioned, high electric power outputs are obtained, thanks to the difference in tribopolarity between ITO and Kapton. Furthermore, Kapton has shown to have high thermal stability (maintains output power of ~ 480 V even at 60 ° C), high tensile strength (234 MPa), and high dielectric strength (240 V / μm) and ITO has a high electrical conductivity (~ 10 S cm). The ITO surface acts as a friction layer against the Kapton film, in addition to be a current-collector for the top layer, which reduces material costs, as well as making a more compact structure.

In summary, this model contains all the data needed to manufacture a one-cell robust U-TENG, in a simple and low-cost way, from commercially available PET / ITO and Kapton electrodes.

6 DETAIL ENGINEERING

6.1 ELECTRIC CIRCUIT MODELLING

There are several types of triboelectric generators. Most of the references differentiate between sliding-mode and parallel contact-mode plates, with in-plane and vertical charge separation, respectively [18, 19] (Hinchet et al., 2018)(Niu & Wang, 2014).

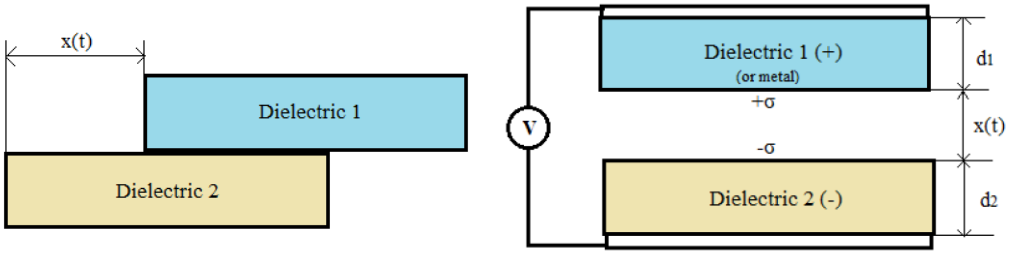

Figure 3: Theoretical models for sliding mode and parallel contact-mode plates. Reproduced from Niu et al. [19] (Niu & Wang, 2014).

In our case we will model the one of parallel contact-mode plates. Specifically, the one that follows the metal-air-dielectric-metal structure.

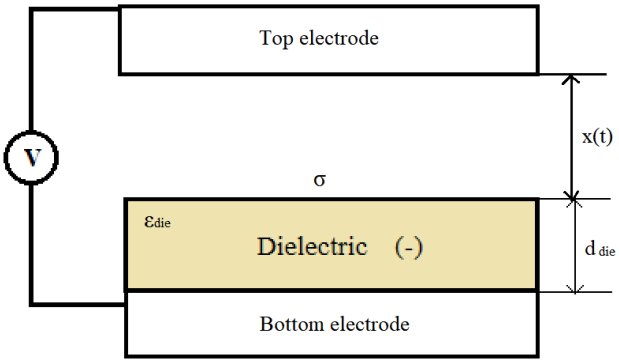

Figure 4: Theoretical models for metal-air-dielectric-metal contact-mode plates. Reproduced from Ronan Hinchet et al. [18] (Hinchet et al., 2018).

A triboelectric, as we observe, has the structure of a capacitance, in which the distance between the electrodes is variable due to a mechanical force. In the case of conductor-to-dielectric type, between the two electrodes we introduce a layer of a dielectric material. The charges will accumulate near the surface and can be characterized with the surface charge density σ. In Figure 4, we also see represented the dielectric electrode layer thickness d_{die} and its permittivity ε_{die}. As regards as the top electrode, the metal layer works also as a triboelectric layer, meanwhile in the bottom, the dielectric layer is the one that works as triboelectric layer and the metal one is the electrode.

The dielectric layer is introduced between the plates, since this material shows a high polarization, so that it acts as an insulator and allows the conductive places to never get in contact. The dielectric increases capacitor capacitance, reducing the electric field strength and therefore the voltage needed to obtain a charge.

The vertical distance between the metal and the air-occupied dielectric corresponds to the distance x(t). A voltage is induced when the electrodes separate from each other, which means that x(t) increases, and this potential difference triggers the charge transfer between the two electrodes. The charge transferred between the two electrodes is defined as Q and the triboelectric layer charge is expressed by means of the surface charge multiplied by the total surface (Sσ). In the top metal layer, as it works as electrode and triboelectric layer, the total charge will be Sσ-Q.

Once the structure of the system is defined, we can discuss its behaviour. As already mentioned, a change in x(t) will induce a voltage in the system. Knowing that x(t) will vary periodically, due to periodic mechanical force, we can deduce that:

- When the distance between both triboelectric surfaces x(t) tends to zero (considering the zero distance as two surfaces in contact), the capacity will be maximum and, therefore, the voltage will tend to zero.

$$x(t) \rightarrow 0;\ C_{TENG} \text{ maximum};\ V_{OC} \rightarrow 0$$

- When the distance x(t) is maximum, the capacity will acquire its minimum value and the voltage its maximum value.

$$x(t) \text{ maximum};\ C_{TENG} \text{ minimum};\ V_{OC} \text{ maximum}$$

According to equation V-Q-x, varying this distance x(t), it also varies potential and load.

$$R\frac{dQ}{dt} = V$$

$$V = -\frac{1}{C_{TENG}}Q + V_{OC}$$

Equation 1: V-Q-X equation described in Niu et al. [19] (Niu & Wang, 2014).

Where C_{TENG} is the capacitance between the two electrodes, which resemble a capacitor, and V_{oc} is an open circuit voltage. Q refers to the charges on the plates of the triboelectric nanogenerator. As indicated in Simiao Niu et al., the terms of this equation will be two elements of the circuit equivalent to the triboelectric generators that we will model and integrate through a Spice type software.

From the equation 1, we model the equivalent electric circuit of the triboelectric nanogenerator, where the voltage source and the capacitor are placed in serial connection. The capacitor will behave as an impedance to the AC voltage source Voc.

The voltage source will be simulated as an ideal voltage source. Since this voltage is caused by the separation of the charges on the plates, it will depend on the x-distance between them. In addition, the capacity will also be defined by the same distance between plates. These dependencies will be discussed later.

In Simiao Niu and Zhon Lin Wang article [20] (Niu et al., 2014), voltage and capacity for parallel plate contact-mode TENGs were defined with the following equations:

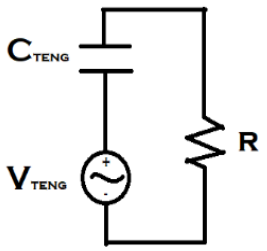

Figure 5: Equivalent circuit model of the triboelectric generator schematic. Based on Niu et al. [19] (Niu & Wang, 2014).

$$V_{TENG} = \frac{\sigma}{\varepsilon_o} x(t) \qquad C_{TENG} = \frac{\varepsilon_o S}{d_0 + x(t)}$$

Equation 2: V_{TENG} and C_{TENG} equations. Defined in Niu et al. [19] (Niu & Wang, 2014). *V_{TENG} described in the equation corresponds to the Voc described in Equation 1.*

Therefore, we need to define the parameters on which the voltage and the capacity depend. These are: the TENG surface S, the dielectric electrode layer thickness d_{die} and its permittivity ε_{die}, the total triboelectric charge Q_{TE} and the triboelectric charge density σ_{TE} (which is placed on the bottom electrode and facing the top electrode). The separation distance x is variable, and this air gap has a permittivity ε_{air}. The parameter d_o corresponds to the effective dielectric thickness and is defined by the expression: $d_0 = \sum_i^n \frac{d_i}{\varepsilon_i}$.

TENG material parameters	
Dielectric (PTFE)	ε_{rdie}=3.4 d_{die}=125 µm
Surface (S)	0.005 m^2
Surface charge density (σ)	−8 µC m^{-2}
Maximum separation distance (x_{max})	0.002 m
Velocity (v)	0.1 m s^{-1}

Table 2: TENG material parameters. Obtained from Ronan Hinchet et al. [18] (Hinchet et al., 2018) *and compared with Niu et al.* [19] (Niu & Wang, 2014).

In the equations defined above (Equation 2), we see that both voltage and capacity depend on the distance x. In the article the distance x was modelled as a simple harmonic movement following this equation:

$$x = \frac{x_{max}}{2} - \frac{x_{max}}{2}\cos\left(\frac{\pi v}{x_{max}} t + \varphi\right)$$

Equation 3: Gap distance x(t) mathematical expression. Defined in Ronan Hinchet et al. [18 (Hinchet et al., 2018)*].*

In order to make a study of the theoretical behaviour of a triboelectric generator we will model it. It can be modelled with Matlab, HDL or PSpice. We will use the last one because of its simplicity and ease of making the interface with the SPICE simulator, type LTSpice, directly.

We will simulate the distance x as a voltage source that emulates displacement. Therefore, when integrating the Voc into LTSpice, we must create a voltage source controlled by voltage, that is, controlled by x. This type of voltage source has analog behaviour and follows a sine shape where the amplitude is x(t). Also, when integrating the capacity, this will become a voltage-controlled capacitor.

6.1.1 **Modelling a voltage-controlled voltage source for V_{OC}(x)**

In order to model voltage-dependent voltage-source, we first look for its definition in the LTSpice Help:

> *Syntax: Exxx n+ n- nc+ nc- <gain>*
>
> *This circuit element asserts an output voltage between the nodes n+ and n- that depends on the input voltage between nodes nc+ and nc-. This is a linearly dependent source specified solely by a constant gain.*

In our case we have a constant gain, since the voltage depends linearly on the distance. Therefore, the gain is $\frac{\sigma}{\varepsilon_o}$. If we take the surface charge density and air permittivity parameters defined in Table 2 [18] (Hinchet et al., 2018) we obtain the following gain:

$$V_{TENG} = \frac{8 \cdot 10^{-6}}{8{,}8541878 \cdot 10^{-12}} x(t) = 9{,}035 \cdot 10^{5}\, x(t)$$

Considering that the maximum distance is 0.002 m, the maximum output voltage (V_{OCMax}) de ≈1807,06 V. With the objective of understanding the behaviour of this voltage source dependent on another voltage source (Voc), we will first do a simulation in which the x signal varies linearly between the zero and the maximum separation distance x_{max} limits.

Based on the definition given above for the separation distance x, we simulate the x-distance as a sinusoidal voltage independent source.

Since LTSpice does not allow us to directly generate a cosine function for voltage, we will work with the sine and a phase. The $\frac{x_{max}}{2}$ term corresponds to the DC Offset. To model it, we take the equation and parameters in Table 2.

$$X(t) = 0.001 - 0.001*\cos(50\pi t) = 0.001 - 0.001*\sin(90 - 50\pi t)$$

$$V = Amplitude * sin(2 * pi * F * t + Phi) + DC\_OFFSET$$

Equation 4: Definition of the voltage that represents the displacement in meters.

As mentioned, this change in distance will be simulated as a change in potential. Therefore, 0.002 meters will be equivalent to 0.002 mV. When matching both expressions, and considering that $\frac{\pi v}{x_{max}} = 2\pi f$, we obtain the terms to introduce in the simulation:

Amplitude = -0.001 mV
F = -25 Hz
Phi = 90º
DC_OFFSET = 0.001 mV

By entering the terms obtained from equation 4 in LTSpice we obtain the following simulation:

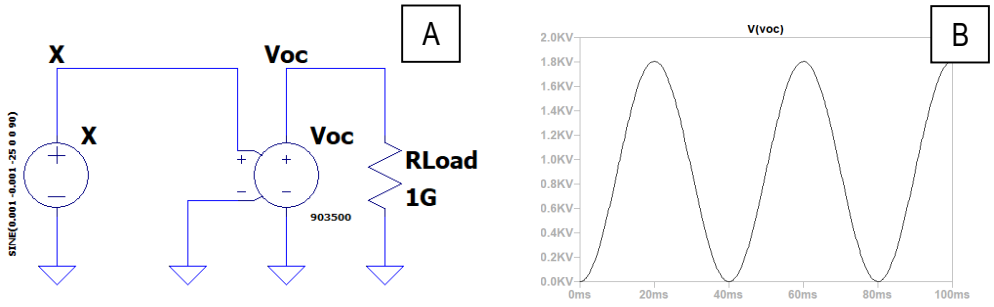

Figure 6: (A) Voltage-controlled voltage source schematic. (B) Transient simulation of Voc.

The open circuit observed has a semi-period of 20 ms, which coincides with the one of the displacement x(t). As the resistor value is fixed, when the x(t) takes its maximum value, 2 mV, it also does the open circuit voltage and the current at Rload, with values of 1.8 kV and 1.8 μA.

In this simulation we have worked with a sine pulse with the frequency obtained from the parameters in Table 2. However, we must keep in mind that our project is contextualized in a biomedical application, in particular, in taking advantage of the heartbeat to mark the motion of the triboelectric plate. The cardiac movement does not exactly match the sine shape with which we have worked, and that is why we should look for the most suitable expression to model the heartbeat as a pulse.

6.1.1.1 Modelling heartbeat as a pulse

The heartbeat is a complex process as it ranges from the excitation due to an activation potential to the refractory period after depolarization of myocardial cells. This process can be measured from different physiological factors: pressure, electrical signal, resonance, vibration, etc. It is clear that a simulation of the heart pulse will never become accurate, as it may approach its shape but will not contemplate possible alterations, arrhythmias or others.

When modelling it, we must bear in mind different features, such as frequency of oscillation, how much the oscillatory rate changes, how does the signal behaviour change within an oscillation, etc. Considering these factors, am adaptive non-harmonic model is defined in Hau-Tieng Wu et. al. [21] (H. T. Wu et al., 2016) to model the pulse signal.

This model uses parameters obtained from observations of the physiological signal and introduces the wave shape function, that models signal oscillation over a period. The article [21] (H. T. Wu et al., 2016) describes a phenomenological model given by the following expression:

$$f(t) = A(t)s(2\pi\phi(t))$$

Equation 5: Intrinsic model type function of the pulse wave signal, where s is a wave shape function, A is a positive differentiable function and ϕ is a monotonically differentiable function.

Despite this would be a more accurate model, we will not use it because of its complexity, as we are more interested in the oscillatory behaviour. For this reason, we will focus on describing the x(t) displacement by associating the cardiac frequency to a characteristic pulse for a given frequency.

Among the studies that discuss the performance of implantable triboelectric nanogenerators for energy harvesting in the heart, in 2019 was proposed the *Symbiotic cardiac pacemaker* [22] (Ouyang et al., 2019). This study seeks to take advantage of the cardiac movement for the displacement of the TENG plates, introducing it between the pericardium and the heart. The energy generated by the TENG is sent, through a rectifier, to a capacity of 100 μF, where the energy is stored and then used to power a pacemaker.
Prior to the implantation of the triboelectric, an in vitro study was carried out. In the in vitro test, the movement of the heart was modelled with a linear motor. The parameters used for this test were:

Frequency = 1Hz
Operating distance = 50 mm
Acceleration/deceleration = 1 m/s^2
Maximum speed = 1 m/s

The defined frequency corresponds to 60 bpm (beats per minute), which approximates to the reference values for a person in rest. This test was followed by an accelerated fatigue test in vitro, to study the damage of materials under cyclic stresses reducing the test time:

Frequency = 100Hz
Operating distance = 1.5 mm

Finally, to make a more realistic simulation of the in vivo environment, the iTENG was placed in a chamber with phosphate buffer saline and the accelerated fatigue test was repeated.

Previously to this study, in 2016, Zhong Lin Wang's team [23] (Zheng et al., 2016) carried out a study to demonstrate the usefulness of implantable triboelectric nanogenerators (iTENG) for in vivo biomechanical energy harvesting.

In the *in vivo* study, the displacement of the plates was driven by the cardiac movement of an adult swine. In this case, the iTENG was connected to a 10 μF capacitor through a rectifier, and aimed to feed a cardiac monitoring device.

In the *in vitro* study, the TENG was driven by a linear motor under different frequency values of the applied force: 0.5, 1, 1.5, 2, 2.5, and 3 Hz. These frequency values are associated to heart rates from 30 to 180 bpm, exceeding the limits of normality. The testing time was 10 s (charging time).

6.1.2 **Modelling a voltage-controlled capacitor C(x)**

As a previous step, in order to define the capacity depending on the voltage in LTSpice, it is important to mention the physics of them. The ability of an electrical charge store (Q) is proportional to the applied voltage (V) and its capacity (C). Therefore, the capacitor charge formula is Q = V * C, with Q measured in Coulombs, V in volts and C in Farads. To introduce this expression in LTSpice we will use the following syntax:

Syntax: Cnnn n1 n2 Q = <expression>

Where the corresponding expression will be the product of the capacitance per x, that means the voltage across the device.

First, we will consider a controlled scenario of capacity variation for a better understanding of its behaviour. In this scenario, we assume a capacity that varies linearly between two limit values (from 1nF to 10nF), depending on an X signal, a voltage. We define this voltage as a PWL function between t=0 x=1 and t=20μs x=10, that is, an X(t) that varies linearly. To test it we will create a circuit in which the capacitor is in serial connection to a known resistance and connected to the rectangular pulse voltage source defined previously.

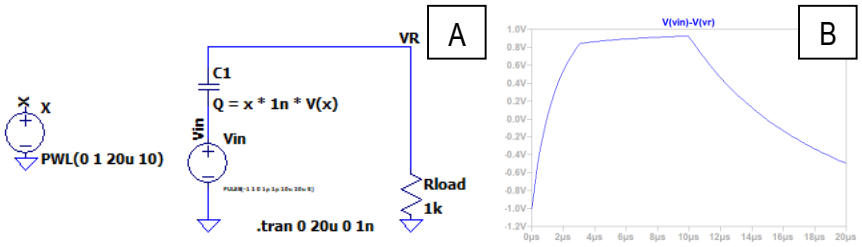

Figure 7: LTSpice schematic of a linearly varying capacitor from 1nF to 10 nF during 20μs (A) and the representation of the voltage difference through the capacitor (Vin – Vr) during this period of time (B).

We observe that it does not give time to the capacitor to get charged completely, as when increasing the capacity, the capacitor load time (T_{load}) increases consequently. Because of that, the capacitor will start discharging before arriving to 1V with a growing discharge time ($T_{discharge}$).

Once we have seen the behaviour of a linearly changing capacitor, we can go back to the TENG modelling. First of all, we will obtain an expression of the C_{TENG} by introducing the parameters of Table 2 in the equation 2.

$$d_o = \frac{d_{die}}{\varepsilon_{rdie}} = \frac{125 \cdot 10^{-6}}{3.4} = 36.76 \cdot 10^{-6}\, m$$

$$C_{TENG} = \frac{8{,}8541878 \cdot 10^{-12} \cdot 0.005}{36.76 \cdot 10^{-6} + x(t)} = \frac{4{,}427 \cdot 10^{-14}}{36.76 \cdot 10^{-6} + x(t)} \quad in\ F\ and\ x(t)\ in\ m$$

Equation 6: Expression of C_{TENG} obtained after substituting the values of the table 2 in the equation 2.

Previously we have discussed that when x(t) equals zero, the triboelectric capacity will be maximum, and that when x(t) is maximum, the capacity acquires its minimum value. From these statements we can obtain:

$$x(t) = 0 \rightarrow C_{TENG,\,MAX} = 1{,}2 \cdot 10^{-9}\ F$$

$$x(t) = 0.002\ m \rightarrow C_{TENG,\,MIN} = 2{,}17 \cdot 10^{-11}\ F$$

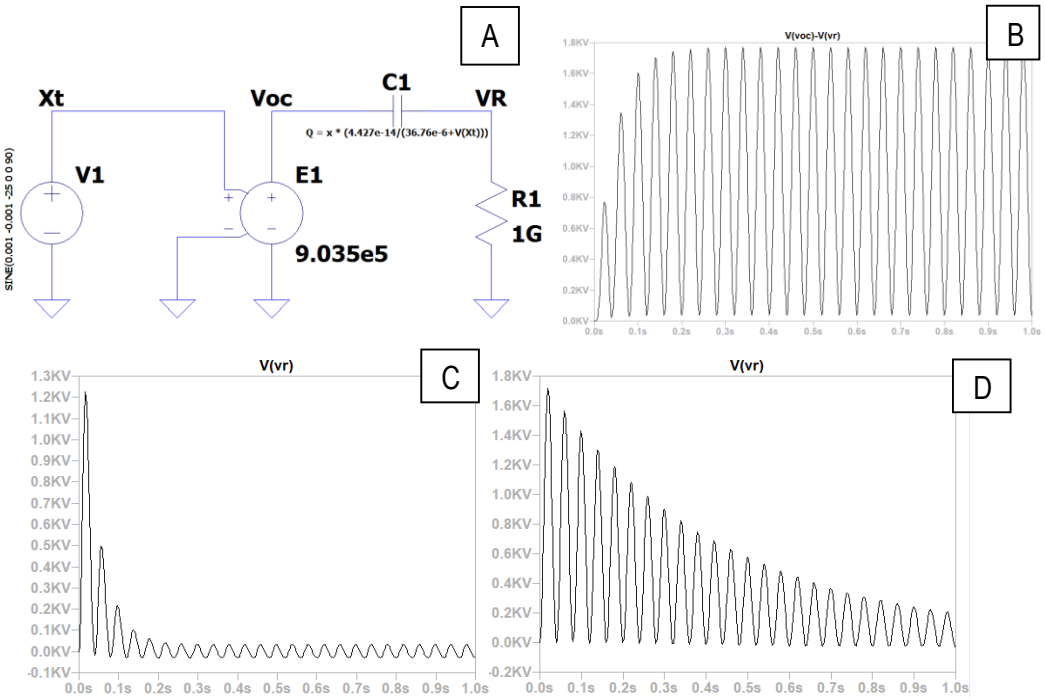

Figure 8: LTSpice schematic of the whole TENG system (A). In B, we observe the capacitor voltage against time. In C and D, the resistance voltage for R1 (Rload) of 1 GΩ and 10 GΩ, respectively.

In this simulation, taking a value of 1 GΩ for Rload we observe that voltage through capacitor Vc tends to 1.8 kV (Figure 8B), that is, when the capacitor is completely charged it acquires a voltage value equal to V_{OCMax}. Moreover, we observe how the voltage through the resistance falls to zero as the capacitor gets charged, as the there is no current through the circuit (Figure 8C). In the case of a Rload or R1 of 10 GΩ (Figure 8D), we observe that the fall in Vr is slower, as a higher resistance means a higher charging time.

When studying the effect of the parameters, we have first analysed the variation of voltage depending on the surface charge density (σ). Depending on the material and the process of making the electrode, the loads will be located inside or on the surface of the dielectric layer and therefore the charge density (σ) will vary [18] (Hinchet et al., 2018).

Basing on V_{TENG} and C_{TENG} equations (Equation 2), we can say that the capacitor value is independent of the value of the charge density. Therefore, this value only will change V_{TENG} value, so that the higher charge density, the higher the voltage reached. In Figure 9, it has been simulated the voltage through the capacitor for two different charge density values. It is observed that, as capacitance value keeps equal, the charging time for both is the same, but the maximum voltage reached increases with charge density, as V_{TENG} also does.

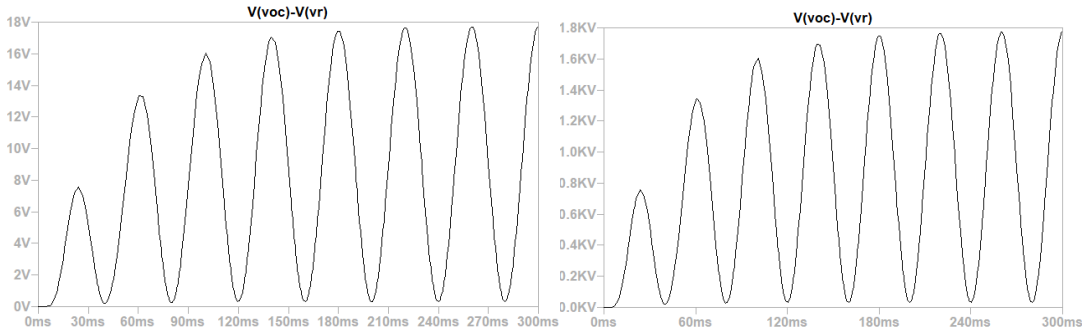

Figure 9: Simulation of the voltage through capacitor against time for σ=8·10^{-8} C/m^2 and σ=8·10^{-6} C/m^2, left and right, respectively.

In order to analyse the effect of Rload, we have simulated the behaviour of the system for a first semi-period, which is 20ms, for different resistance values. As could be expected, when the resistance increases, the intensity circulating through the resistor decreases. Also, when we decrease the resistance we notice that the peak value of the voltage also drops.

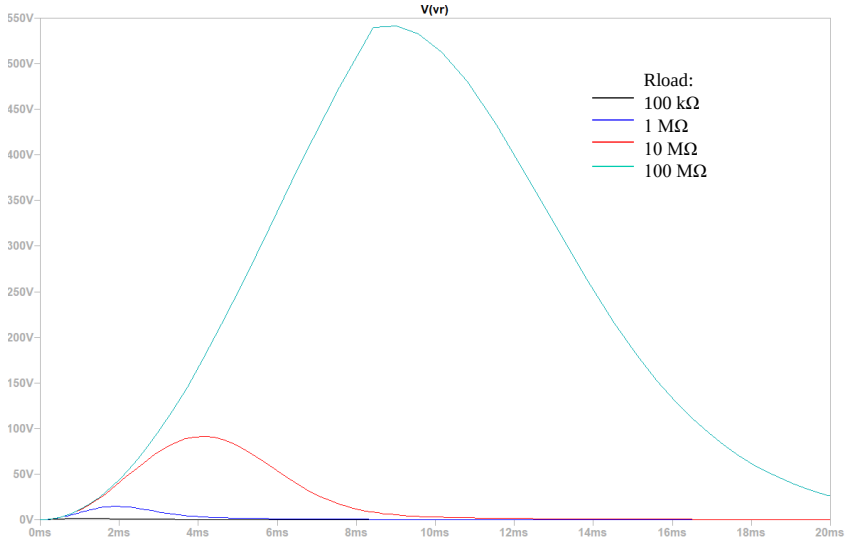

Figure 10: Voltage through the resistor against time for different values of Rload.

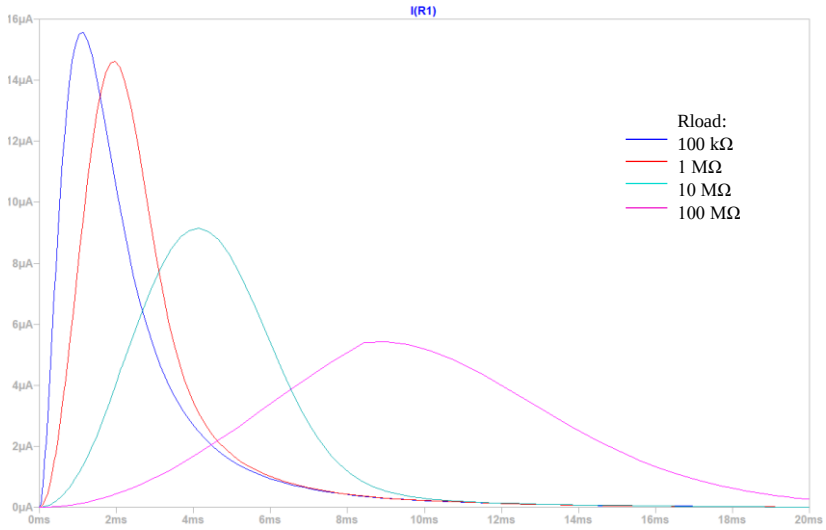

Figure 11: Current at the resistor against time for different values of Rload.

In Figure 10, we have represented the voltage in the resistance. From this representation, we can obtain which is the behaviour of the charge peak, as when the resistor voltage increases, the voltage through the capacitor decreases and, consequently, the charge in the capacitor also decreases. Therefore, for a very small resistance, ideally zero, we will have the maximum load peak for our capacity. For higher resistances, we see the effect of the RC constant.

It is therefore of special interest to represent the influence of the resistance on the output current and voltage. To do this, we will take the maximum values of intensity and voltage for different resistance values, obtain curves through interpolation and plot them. In Figure 12C, we can observe the relationship between power and load resistance, and in this way obtain the optimum resistance for the TENG parameters previously discussed. We observe a maximum output power peak of approximately 2.92mW for a load resistance value of 100 MΩ.

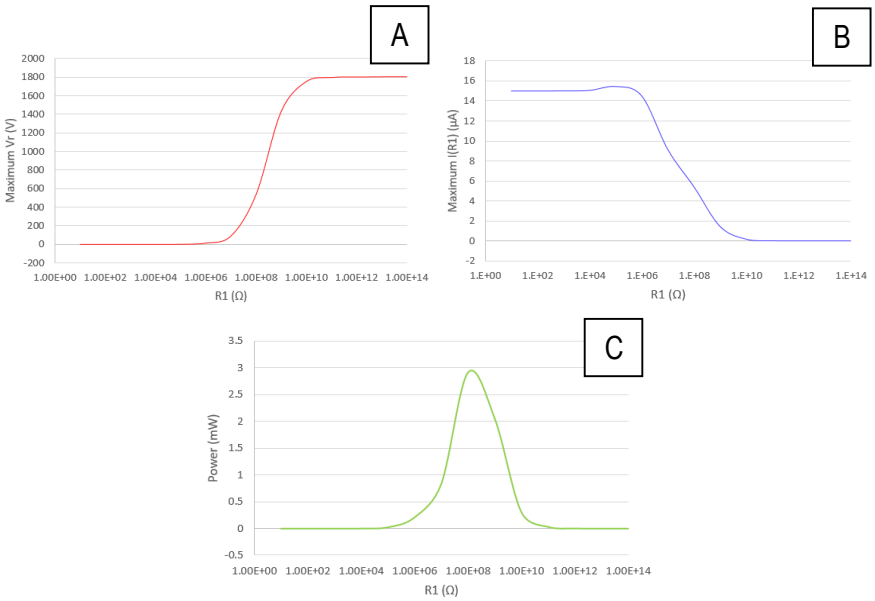

Figure 12: Voltage (A), current (B) and power (C) variation depending on Rload.

Therefore, the modelled TENG exhibits:

Table 3: Summary of power and tension values	
Maximum open-circuit voltage ($V_{oc,MAX}$)	1.8 kV
Maximum output power peak (R_{load} = 100 MΩ)	2.92 mW
Power density (R_{load} = 100 MΩ and S = 0.005 m^2)	584 mW / m^2

Table 3: Summary of power and tension values

6.2 POWER MANAGEMENT CIRCUITS

6.2.1 AC/DC rectifier circuit

So far we have modelled the behaviour of our triboelectric with respect to ground, and we have seen that it is a time-varying signal that approximates to a sinusoidal signal. Actually, the signal inside the body would be differential, and that is why our system must work with respect to a floating reference, and not with respect to the ground.

As discussed, the TENG gives as an output a very unstable AC signal. As it is not desirable for multiple applications, in order to recover energy, we will use power management circuits. An example of a system that converts AC outputs to DC outputs is a rectifier bridge.

With power management circuits, the energy generated by the TENG is stored in a capacitor through a rectifier. This stored energy can be used to feed an external electronic circuit with a specific function, as the capacitor charge behaves as a battery.

First, it has been simulated a simple model with rectifier circuits to later move on to advanced rectifier circuits [24] (Santiago Rodriguez, Garraud, Alabi, Garraud, & Arnold, 2019). Based on Nanoenergy 2014 [20] (Niu et al., 2014), our first approach is a diode bridge rectifier, and a Rload and CLoad with fixed values, 100 KΩ and 10 µF, respectively, that are parallel connected. To define the floating reference, a very high resistance is introduced, 100.1 GΩ, that connects the circuit to ground.

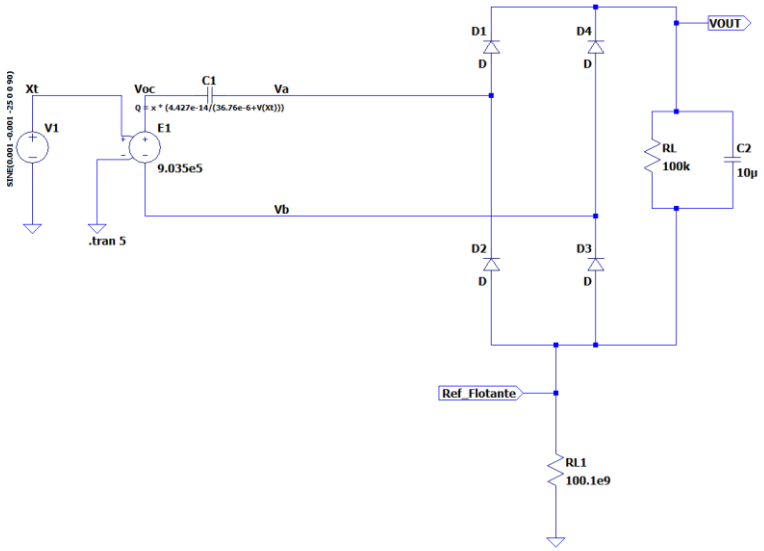

Figure 13: Power management circuit formed by a diode bridge rectifier and a RL and CL (or C2) parallel connected.

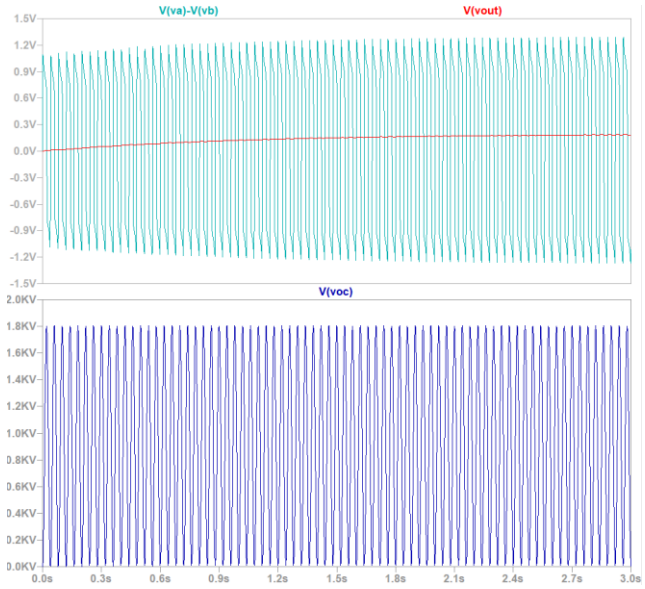

Figure 14: At the top, representation of V(va)-V(vb) input signal and Vout signal against time. At the bottom, representation of Voc (open-circuit voltage) against time. R_L = 100KΩ and C_L = 10µF.

As we observe in Figure 14, we have a periodic noisy signal in AC (*V(va)-V(vb)*) that, when introduced in the power management circuit with the given reference conditions, gives a 200mV DC output signal (*Vout*), approximately.

To study the behaviour of the output voltage, we give different values to R_L and C_L, and see the output dependency on these two parameters. When comparing Figures 15A and 15B, we observe the effect of R_L. As we decrease the value of the R_L, the DC voltage signal also drops., and ripple increases. However, by decreasing the C_L value, we do not have a voltage fall and only increase the ripple.

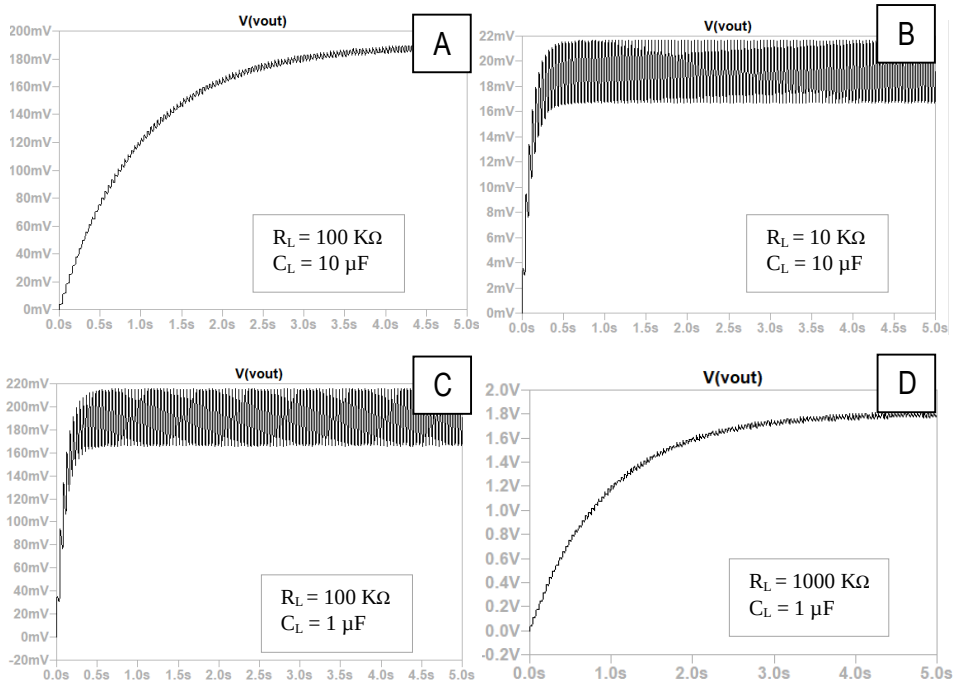

Figure 15: Vout against time representation; (A) for R_L = 100 KΩ and C_L = 10 µF, (B) for R_L=10 KΩ and C_L = 10 µF, (C) for R_L = 100 KΩ and C_L = 1 µF and (D) for R_L = 1000 KΩ and C_L = 1 µF.

In the simulations shown in Figure 15, we observe how the signal ripple depends on C_L, which acts as a filter, so that a higher value of C_L sets a lower voltage ripple. In Figure 15D, we see that when the R_L takes large values, V_{out} behaves as a DC signal. Moreover, for high values of R_L, we observe that a change in C_L does not affect the DC voltage, and this is due to the fact that a capability behaves like an infinite impedance to a DC current, and being parallel to a resistor, the total equivalent impedance will depend only on R_L.

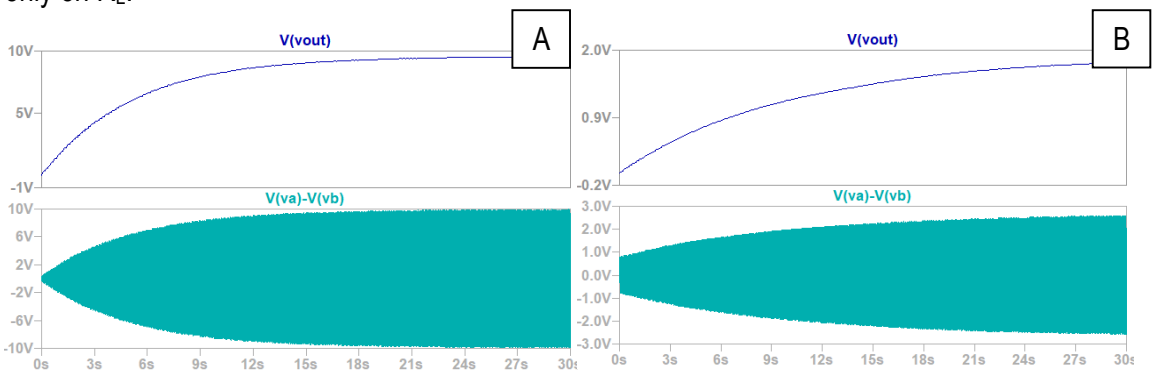

Figure 16: Transient simulation for (A) R = 10MΩ y C = 1µF, (B) R = 1MΩ y C = 10 µF.

DC current and voltage are limited by Rload. This load resistor asks for more or less current depending on its value and, consequently, V(va)-V(vb) is also modified.

As the C_L will have little effect on V_{DC}, it will only be necessary to define an optimal R_L for which we will obtain the largest average DC power. With this purpose, we have studied more deeply the influence of the load charge with a fixed value of C_L of 1 µF. In Figure 17C, optimization of the performance of the TENG as function of R_L has been discussed, by obtaining average output power profile from the average voltage and current for different load resistances (Figure 17). We observe that the maximum average output value is obtained when R_L is 10 MΩ, and this peak reaches 14.2µW.

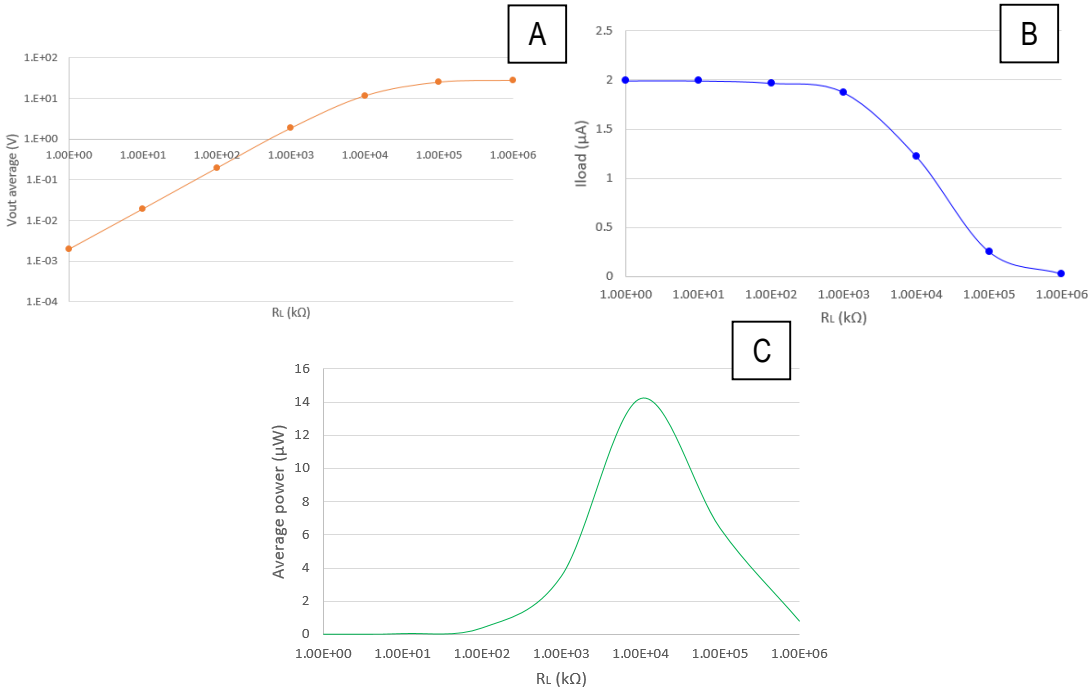

Figure 17: Average Vout and average current at Rload versus Rload, A and B, respectively. In C, derived curve for average output power versus Rload.

To advance in the studio, the input power performance as function of the load resistor has also been discussed. For this, the input current and input voltage (Va-Vb) have been simulated for different values of Rload. In Figure 18, we observe an AC voltage and a current with a shape different from a sinusoidal one due to the harmonics.

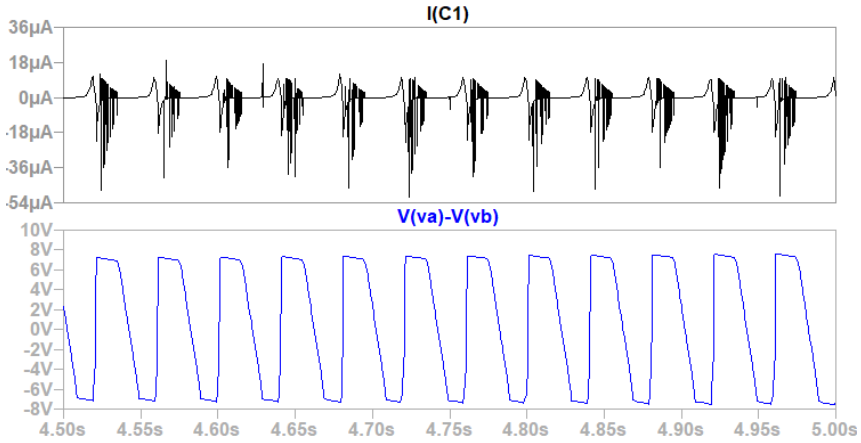

Figure 18: Input current and voltage for a Rload of 10 MΩ.

By multiplying both, we would obtain the instantaneous power. In order to obtain a single value of input power for each Rload, we have made the product of the RMS values of both intensity and voltage. The ratio of the output and input power gives us the efficiency of our circuit, shown in Figure 19.

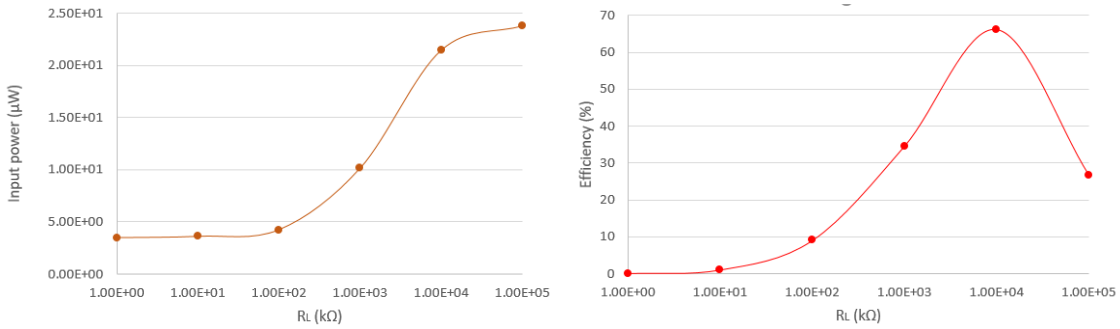

Figure 19: Dependence of the input power and efficiency percentage on Rload, left and right, respectively.

This single phase rectifier gives us an AC input and a DC output, from which we have obtained RMS power value and the average power, respectively. Fixing a R_L value of 10 MΩ, which is the optimum value, we obtain a RMS input power of 23.2 µW. Therefore, this specific power management circuit has an efficiency of 66.2%, a very low value.

DIODE BRIDGE RECTIFIER (R = 10MΩ AND C=1µF)

	Voltage	Current	Power
INPUT	6.3 V (RMS)	3.6 µA (RMS)	23.2 µW
OUTPUT	11.6 V	1.22 µA	14.2 µW
EFFICIENCY	~ 66.2%		

Table 4: Efficiency analysis of the diode bridge rectifier (R = 10MΩ AND C=1µF).

A further study has been carried out in order to study if this low efficiency was triggered by the voltage drop of the diodes. On a diode bridge there are always two forward diodes, so since each diode needs 0.7 V (conventional silicon diodes), together they take 1.4V, voltage that we are losing. As the input voltage increases, the voltage drop in the rectifier becomes less significant in proportion, that is why this circuit has an efficiency proportional to its input voltage. Therefore, a general way to enhance the performance is introducing a diode with less voltage drop. An example of a very low drop diode is Schottky diodes, which have a threshold voltage of approximately 0.2 V to 0.4 V.

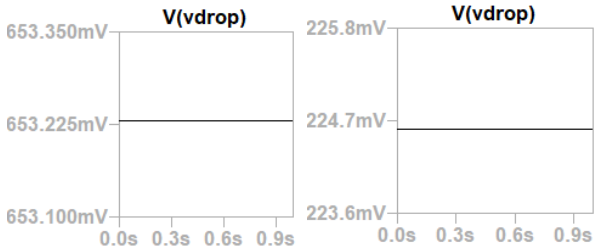

Figure 20: Simulation the voltage drop at of a silicon type diode (left) and a Schottky type diode (bottom). The silicon type diode (model 1N914,) shows a forward voltage drop of 653,2mV. The Schottky diode (model MBR0530L) shows a voltage drop of 224.6 mV.

However, when comparing the performance of four different diode types, two silicon types (1N1914 and MURS120) and two Schottky (CMDSH2-3 ans RB058L_40), there is no evident change in efficiency. Therefore, more advanced electronic configuration methods will be necessary to improve the efficiency of the system.

6.2.2 TENGs stack

It has been reported that one way to obtain a higher output power while maintaining the device area is by vertically stacking of several triboelectric generators [25] (Seol et al., 2015). In the study of Seol et. al., each TENG is made up of three electrodes: the upper and lower electrodes act as anodes, inside the encapsulation formed by the two anodic electrodes we find a vibrating membrane that contains the cathodic electrode inside. In the resulting structure, the anode electrodes were connected to each other and the cathode electrodes were also connected to each other, therefore TENGs connected in parallel are obtained.

Therefore, a parallel TENG configuration is proposed. In this way, total area keeps constant, which results of special interest as we must adapt to size limitations for bioengineering applications. The resulting structure, based on our TENG model, is shown in figure 21.

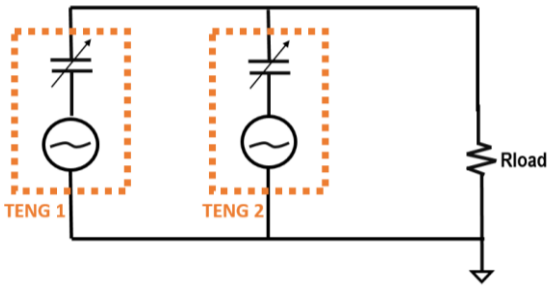

Figure 21: Schematic of the resulting structure model.

To see if this configuration actually involves an improvement in output we have simulated the behaviour in LTSPICE. Firstly, a schematic with two separated TENGs has been generated in order to study them individually. We observe a peak of voltage at 1.175 kV and at the same time a peak of current at 1.36 µA, which correspond to a peak of power of 1.6 mW.

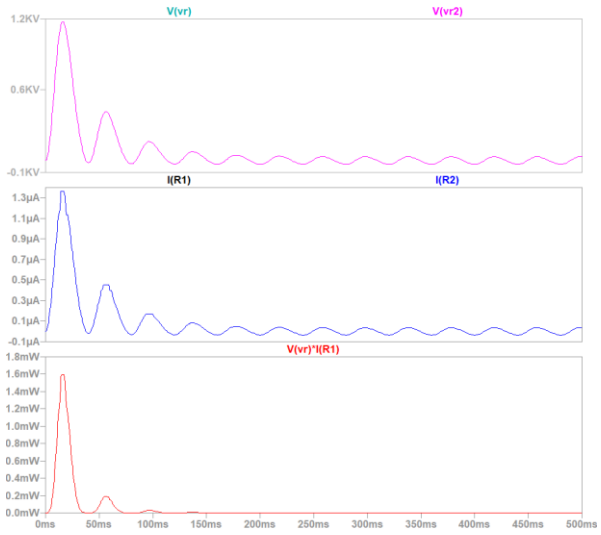

Figure 22: LTSpice simulation of voltage, current and power at Rload of two individual triboelectric generators (Rload = 1GΩ).

If we perform the simulation of both TENGs in parallel, with the configuration defined in Figure 21, and we give Rload a value of 500 MΩ, which is the equivalent resistance of two Rloads in parallel, a power peak of almost 3 mW is reached, with voltage and current values of 1.2 mV and 2.5 µA, respectively. We observe that, as we are working with parallel connected voltage sources, the voltage does not vary while the current is doubled.

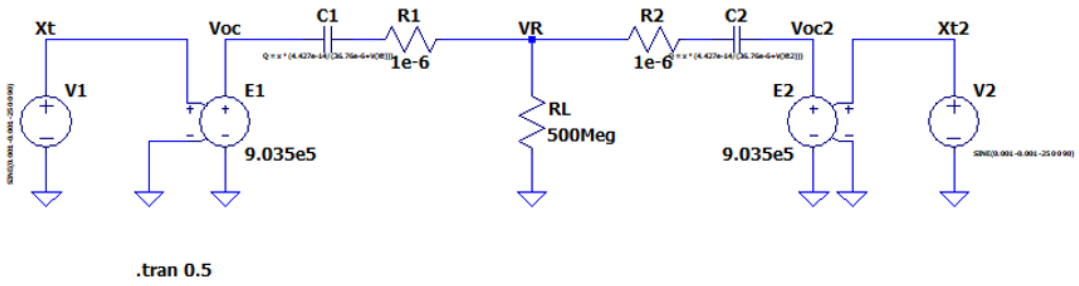

Figure 23: LTSpice schematic of two triboelectric generators parallel connected with a unique load resistance of 500MΩ.

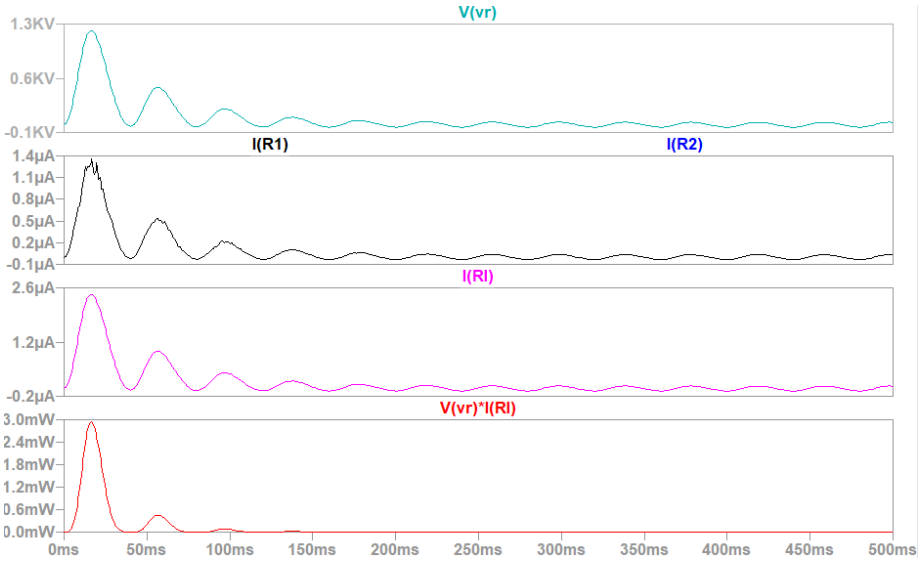

Figure 24: LTSpice simulation of voltage, current and power at Rload of two triboelectric generators parallel connected (Rload = 500MΩ).

Therefore, by parallel stacking two triboelectric generators, output electric power is doubled, as currents are added and voltage does not vary. Consequently, by stacking more than two TENGs, electric power will keep increasing proportionally to the number of TENGs stacked. However, we must bear in mind that, although parallel stacking is the preferred option for stacking as total area is kept, it causes an increase of the total current, which is the most important factor when talking about electric risk, as it will be discussed in chapter 6.4.

6.3 EXPERIMENTAL SET-UP

6.3.1 U-TENG fabrication

As mentioned above, have reproduced the metal-air-dielectric-metal model of parallel contact plates. Specifically, we have manufactured the ultra-simple TENG (U-TENG) described in Mallineni et. al. [1].

The materials used for the fabrication are commercially available and low-cost. The U-TENG is constructed with Indium tin oxide (ITO), an alloy that forms the conducting part of our electrodes, Polyethylene terephthalate (PET), a plastic polymer, and Kapton, a polyamide resistant to high temperatures that acts as the dielectric layer.

For top and bottom electrodes, we have used PET sheets that are coated with ITO in one side, which will be facing the inner part. As a dielectric material we have used Kapton adhesive tape, which has been attached to the bottom electrode. The dimensions of the electrodes are 3.5cm x 2.75cm.

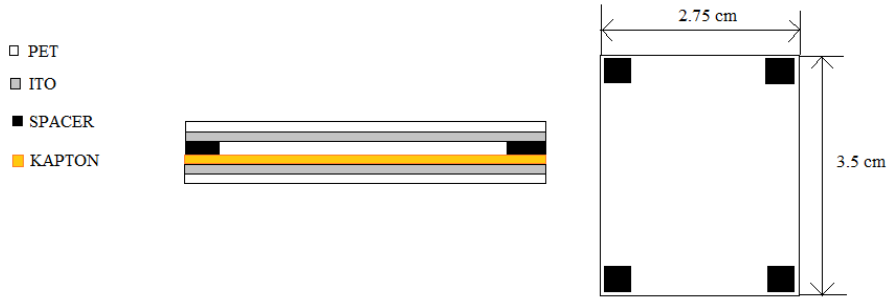

Figure 25: Schematic of the fabricated U-TENG, profile and top view. Based on Figure 3 of Mallineni et. al. [1].

ITO is a liquid metal that, in this structure, behaves as triboelectric material and electrode, while Kapton behaves as the other triboelectric layer, which is negatively charged. Therefore, liquid-solid friction is obtained, which has better contact effectiveness than solid-solid friction due to material roughness, as the solid material is moved in and out the liquid during the operation.

The described model has been designed in SolidWorks, a CAD software for 2D and 3D mechanical modelling:

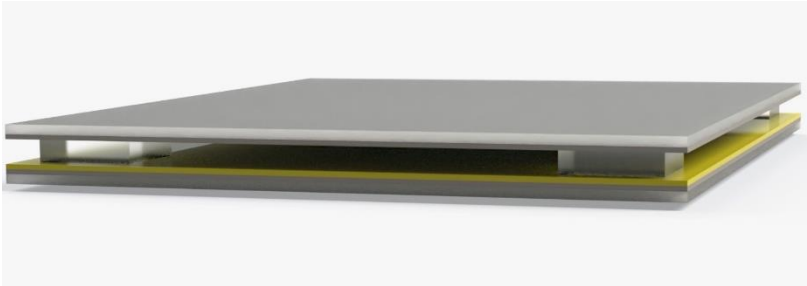

Figure 26: 3D model of the fabricated U-TENG. Performed with SolidWorks software.

All the materials used are low cost and commercially available. It has been used ITO coated PET Plastic from Adafruit, which is coated with an ITO layer on one side, has a thickness of 0.175 mm and shows a resistance of 7.75 Ω per cm^2, as described in the technical details given by the manufacturer.

Moreover, insulating Pyrex separators, of approximate dimensions of 4 mm x 4mm x 1mm, have been used to maintain an air gap between the two layers. Therefore, the distribution will be PET-ITO-AIR-KAPTON-ITO-PET. Finally, Cu wires have been used to connect the electrodes, attached on the edges of the ITO face of the electrodes, as it is the conducting side.

If we refer to the process of preparing the materials, this process is composed by: acquisition, shaping and assembly. The acquisition of the products is detailed in the economic viability chapter, where the providers are mentioned. The materials were shaped and cut with the dimensions described above. For cutting the Pyrex spacers, a glass cutter has been used.

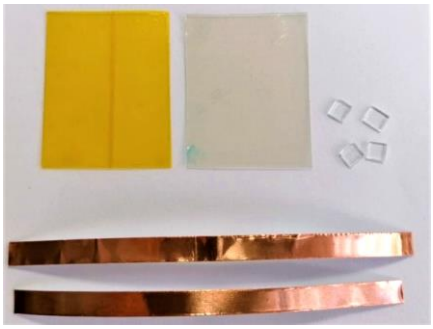

Figure 27: Materials preparation. At the top, from left to right: PET-ITO already covered with the Kapton tape, PET-ITO, and the four Pyrex spacers. At the bottom, the two Cu Wires.

Figure 28: Manufactured U-TENG, profile and top view.

In the modelling section, we have taken a surface area value of 50 cm^2, while the surface area of the U-TENG is much lower. Moreover, the maximum separation distance between plates has been defined as 2mm in the model, while the separators used for the fabrication are 1mm thick. However, as plates are made of flexible materials, the distance between them can vary beyond the spacers, so this difference is not so significant. Therefore, the previous study allows us to understand the electric behaviour of triboelectric generators, but the values obtained will not be shared with the fabrication.

6.4 STUDY OF THE PERFORMANCE OF THE TENG IN BIOENGINEERING APPLICATIONS

The purpose of this research project is to study triboelectric generators performance as energy harvesters, and specifically to study the application of TENGs in the field of biomedical implantable devices, so we need to know their power and voltage requirements. In general, these devices do not need a high value of power supply, it uses to be in a range of microwatts and milliwatts, and voltage requirements around 2 and 3V [26] (Zhao et al., 2020). It is worth mentioning that the supplies for these implantable devices have limitations such as size, compatibility of the material and electric security.

Table 5: Biomedical implantable devices

Cardiac implant	8-190 µW
Cochlear implant	5 - 40 mW
Retinal implant	30 µW – 5 mW
Drug pump	100 µW – 2mW
Neural implant	30 µW – 23 mW
Muscle stimulator	1.3 mW

Table 5: Examples of biomedical implantable devices and its power supply levels [26, 27] (Zhao et al., 2020)(Cadei, Dionisi, Sardini, & Serpelloni, 2014).

Currently, the main way to power these devices is through the use of batteries. However, given its limited lifespan, research is being carried out on transducers to obtain electric power from the human body itself. Apart from triboelectric generators, among the applicable energy harvesters for implantable devices, we find: piezoelectric generators, biofuel cells, thermal electric generators, photovoltaic cells and radiofrequency harvesters [26] (Zhao et al., 2020).

Table 6: Alternative energy harvesting technologies

Piezoelectric generators	0.4 – 30 µW / mm^2
Biofuel cells	0.5 – 13 µW / mm^2
Thermal electric generators	0.4 – 100 µW / mm^2
Radiofrequency harvesters	0.1 – 200 µW / mm^2
Photovoltaic cells	10 – 200 µW / mm^2
U-TENG [1]	4.9 µW / mm^2

Table 6: Power values obtained from alternative energy harvesting technologies [26] (Zhao et al., 2020).

By comparing the values of table 5 with those of table 6, we can affirm that the different energy harvesting methods mentioned meet the supply requirements of the most used implantable medical devices. Therefore, all of them seem to be a valid option for self-feeding medical implants, without the need of any battery.

Despite this, most of these technologies are limited due to their large size, since the power will depend on the surface of the device. In the case of medical implantable devices, energy harvesting devices must be limited in size, as they must be implanted: around 1 cm^3 [27] (Cadei et al., 2014). In addition, the energy obtained in all of them will be unstable and will require accommodation circuits, integrated in

flexible electronics. All these devices must be embedded in a flexible and biocompatible encapsulation, that must try to not affect the performance of the energy harvesting device.

One of the main advantages of triboelectric generators, as well as other energy harvesting technologies, is the low intensity of the electrical current, as it is the most important parameter to quantify the electrical risk. It is important that the body does not get in contact with currents greater than 10 mA [28] (Fish & Geddes, 2009), and as it has been discussed, current takes values of microamperes, so the electric risk is widely reduced.

Since TENGs are mechanical harvesters, they can obtain energy from different physiological movements of the human body. Among the possible sources we find: muscle contraction and relaxation, cardiac and lung motion or blood circulation.

One of the features that make triboelectric generators an ideal candidate for biomedical applications is the wide range of materials with which they can be assembled, since almost all kinds of materials (metal, polymers, wood, etc.) show triboelectrification effect [29] (Zheng, Shi, Li, & Wang, 2017). Among the possible materials, we can choose between those that have the optimal characteristics for its application, such as flexibility, biocompatibility and mechanical properties. Furthermore, most of these materials are commercially available and inexpensive.

In addition, the good performance of the use of biodegradable materials for the manufacture of TENGs (BD-TENGs) has also been demonstrated. Wen et. al [30], talks about the use of silk fibroin film as a good biocompatible and biodegradable strategy for the construction of flexible electronics. BD-TENG was implanted in sub-dermal region, and after some time it was dissolved without leaving any residue.

Several studies have been carried out in order to demonstrate the application of TENGs in implantable form. This is the case of the study by Zheng et. al. [31], in which an implantable triboelectric nanogenerator (iTENG) was implanted in a living rat to harness its breathing motion to obtain energy. Encapsulation was necessary in order to protect the triboelectric structure from the physiological environment.

Apart from power supplying, triboelectric nanogenerators can be used as a sensor to detect small changes of motions inside our body. Ye Ma et. al. [32], proposes an implantable triboelectric active sensor (iTEAS), that allows continue monitoring of several physiological and pathological signals. This self-powered sensor, enables the real-time detection of cardiac arrhythmias, monitoring of respiratory and heart rates and others, reaching an accuracy of ∼99%. In response to the heartbeat, an open-circuit voltage (VOC) of ∼10 V and a short-circuit current (ISC) of ∼4 μA can be obtained.

6.4.1 Cardiac motion and self-powered implantable devices

Among all the possible body movements from which we can transduce mechanical energy to electric energy, such as breathing or motion in human joints, we will focus on cardiac motion. With this purpose, we will simulate the movement of the heart as our source of tension. That is why we are interested in the movement having the maximum similarities with the heart rate (we will simulate in a sinusoidal way) and the behaviour of the heart, as if the triboelectric were located on the surface of the same.

Assuming an average heartbeat of 60 bpm (beats per minute), the heart works at a fundamental heartbeat rate of 1 Hz. Therefore, this will be the frequency with which we will work in order to emulate the cardiac frequency at rest. Increasing the velocity of motion is equivalent of increasing the frequency of the AC

voltage source V_{OC} and, therefore, decreasing the impedance of the C_{TENG}. By increasing the frequency, the matching resistance is lowered and, consequently, the voltage value obtained is higher.

As a first approach, it has been developed an analysis simulation with the same circuit as the one used in the modelling section, with the parameters of Table 2, and operative conditions of R_{LOAD} of 10MΩ and C_{LOAD} 1μF, as these have been discussed to be the optimum values.

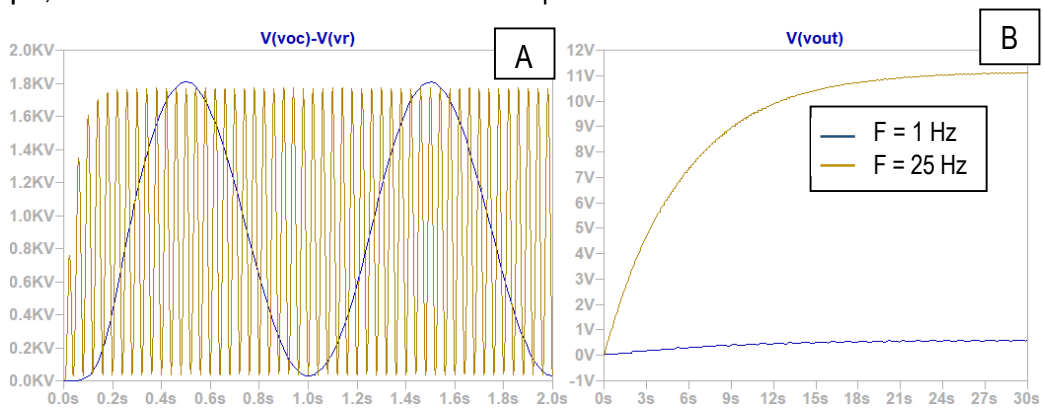

Figure 29: Transient simulation of (A) Open Circuit Voltage and (B) Output Voltage after the rectifier circuit.

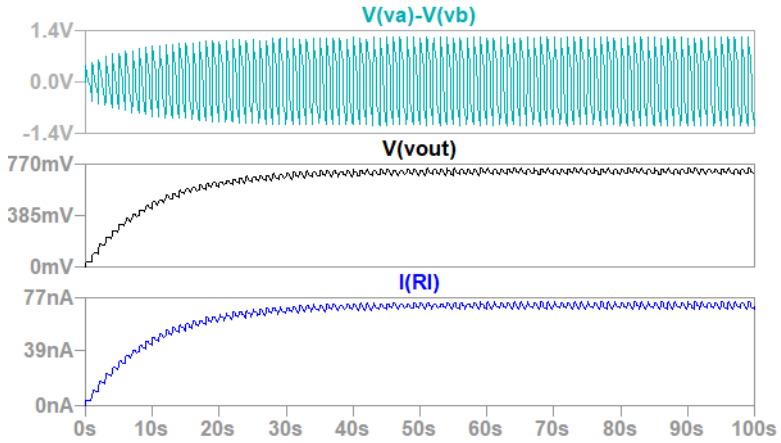

Figure 30: Simulation of the input and output tension in a rectifier circuit for f = 1Hz, R_{LOAD} =10MΩ and C_{LOAD} = 1nF. At the bottom, current at Rload.

	VOLTAGE	CURRENT	POWER
INPUT VALUES	850 mV (RMS)	160 nA (RMS)	136 nW
OUTPUT VALUES	715 mV	71.5 nA	51 nW

Table 7: Input and output values for the rectifier circuit. TENG working at a frequency f = 1Hz, R_{LOAD}=10MΩ and C_{LOAD} = 1nF.

We observe that the output power is decreased with frequency, as the output voltage is also lowered. For a frequency of 1Hz, and the resistor and capacitor values described, an output voltage of 715mV in DC and an output power of 51nW are obtained. Although an optimal voltage is obtained, the output power would not meet the supply requirements for a cardiac implant, defined in table 5. Therefore, implementation of the electronics for energy storage, together with the development of strategies for a better triboelectric performance, appear as new challenge.

7 U-TENG EXPERIMENTAL VALIDATION

This chapter aims to evaluate the performance of the manufactured device by an experimental validation process.

In the first place, before assembling, the electrical continuity of the electrodes, which is the face of PET coated with ITO, has been checked. For the manufacture, two sheets of ITO-coated PET were purchased and none of them gave the same resistance results shown in the technical details, so that it seemed to be non-conductive. Since an infinite resistance does not appear between the two probes, as occurs when measuring insulating materials, we can say that it shows a very low conductivity.

Moreover, continuity has also been looked at in the Cu wires, which show conductivity on the side where the copper is exposed and not on the side that is covered by the adhesive layer. Cu wires have been bent, so that both sides are conductive. After assembling, it has been shown that there is conductivity between the wires and the ITO, although it is low, due to the low conductivity of the ITO. Finally, Kapton, Pyrex and PET have shown to be good insulators as expected.

Once the material properties have been checked, we can proceed to study the U-TENG performance. As we have modelled, we will have two different materials assembled face to face, with an electrode in the back side of the isolating material. In terms of experimental development and characterization, the potential differences come from friction between the two materials. By applying a mechanical force periodically, the spacing between the plates varies and, therefore, the following steps will take place cyclically:

1. When the two materials are in contact, opposite static charges appear on the inner surface of the triboelectric layers.
2. As materials separate a potential difference is created, and charges go from one electrode to the other through an external circuit (where the voltmeter is placed).

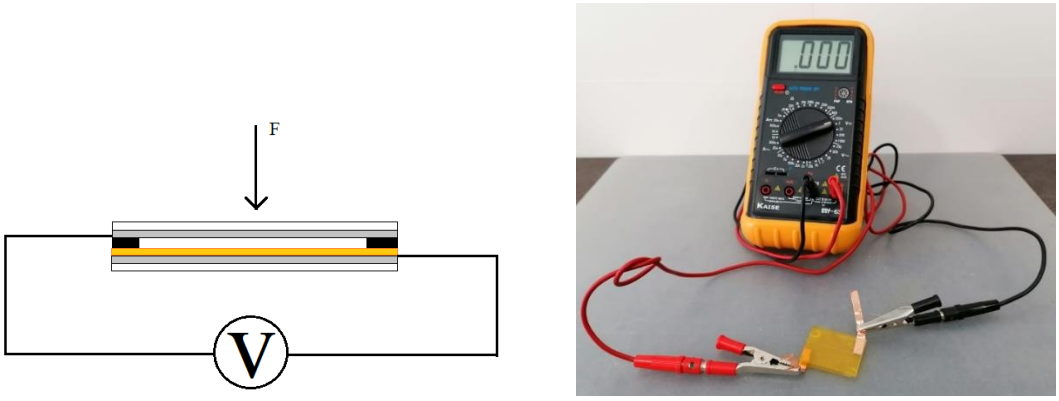

Figure 31: Experimental set-up.

This periodic force has been applied with the finger, covered with a glove so that charges do not escape. The top electrode has been pushed against the bottom electrode once per second (frequency of 1Hz). The electrical measurements have been carried out with a digital multimeter from Kaise.

By applying a periodic force with the fingers, a varying DC voltage has been measured. The open load voltage measured has reached peaks up to 1.071 V, which is the maximum peak voltage obtained. Therefore, it has been shown that the U-TENG works and that a tension is recovered but at levels much lower than expected.

The great differences between simulation and experimental may be related to the methodology in the process. Due to this, it would be advisable to standardize more the triboelectric manufacturing process.

One of the main limitations that causes that the simulation resulting values do not coincide with those measured experimentally is that not all the surface is in contact when testing its performance, as the contact surface coincides with the area of the pusher, i.e. the finger. Consequently, the charges are not equally distributed and the equivalent surface is smaller than the theoretical one. Therefore, the surface on which we should base on our study is the area that is in contact when applying the force. Moreover, as friction is not homogeneous, the electrostatic phenomena does not take place in the same way in all the parts of the plates.

When applying the force with the finger, neither the modulus of the force nor the contact area remain constant, as they may vary slightly in each cycle. Also, periodicity is not granted. Therefore, making use of a pushing tester, instead of applying force with the finger, may lead to a more stable output signal.

It is worth to discuss the effect of area, as the higher the surface the higher the charges that are generated and, consequently, the higher the voltage obtained. With the main aim of observing this effect, triboelectric generators with dimensions 3.5cmx5.5cm and 5.5cmx7cm, which duplicate and quadruple the original size, have been developed. It has been observed a maximum open load voltage of 2.69V and 5.3V, for surfaces of 19.25 cm^2 and 38.5 cm^2.

Therefore, it has been observed linearity between surface and the voltage peaks obtained, as shown in Figure 32. From this we can conclude that in order to optimize triboelectric output surface, increasing effective area is a good strategy.

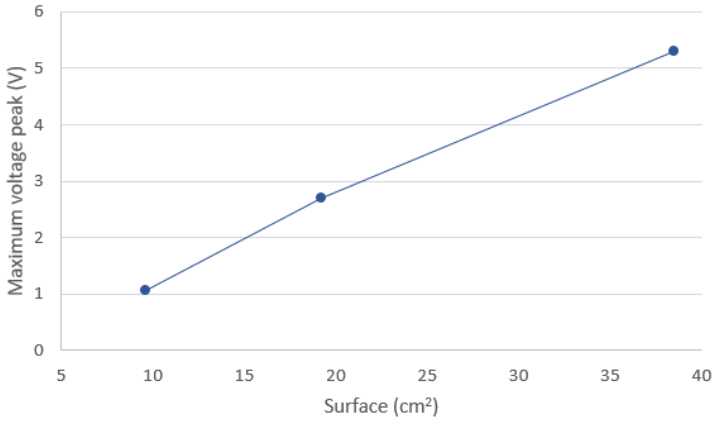

Figure 32: Experimental plot of the maximum voltage peak measured against surface.

The tensions measured with the voltmeter correspond to the open circuit voltage, which was described in Equation 2 as $V_{OC} = \frac{\sigma}{\varepsilon_o} x(t)$. This output tension reaches its peak value when the distance x(t) is maximum. The current operating conditions of the laboratory do not provide a proper way to extract the charge density of our U-TENG. Therefore, in order to obtain a value of the equivalent surface charge density (σ), we consider that the maximum distance between plates is the thickness of the Pyrex separators (1mm), and that it does not depend on the surface, so we can relate them to the maximum peaks measured for each U-TENG constructed (Table 8).

Surface	*Maximum voltage peak*	*Equivalent surface charge density*
9.625 cm²	1.071 V	9.5 nC/m²
19.25 cm²	2.69 V	23.8 nC/m²
38.5 cm²	5.3 V	46.9 nC/m²

Table 8: Summary of the maximum voltage peaks measured for different TENG areas and the calculated equivalent surface charge density.

Although the same materials have been used for each triboelectric manufactured, we observe that the equivalent sigma keeps proportionality with the voltage peak and surface. From the results obtained we can deduce that conductivity does depend on surface, and the lower the surface the lower the conductivity. Proportionality between surface and Voc_{max} has been experimentally demonstrated, which may suggest that Equation 2 should be adjusted to show the dependence of peak voltage or charge density on surface. However, we must bear in mind that we have considered that the distance x(t) reached does not depend on surface, which is not an accurate assumption as plates are very flexible and their deformation may overpass the thickness of the separators. Higher surfaces may deform more and, consequently, increase the maximum distance between plates (x_{max}).

Once the voltage peaks have been measured and equivalent surface charge density has been calculated for each manufactured triboelectric, we could model it and simulate which would be its output power and voltage values under specific conditions, in order to assess the performance of our triboelectric generation in bioengineering applications. To do it, we have selected the manufactured triboelectric with the smaller surface (9.625 cm²) and its respective equivalent surface charge, which is 9.5 nC/m², as we must bear in mind that one of the main limitations of implantable medical devices is their size.

Again, we have contextualized our simulations in cardiac motion energy harvesting, so the frequency of the movement of x(t) is set to 1 Hz, and its amplitude to 1mm, as it is the thickness of the Pyrex separator. As far as the material parameters, the dielectric constant and dielectric permittivity used are the ones described in Table 2 by Ronan Hinchet et. al. [18] (Hinchet et al., 2018). For these parameters, the voltage and capacitor expressions are: $V_{TENG} = 1072.94\, x(t)$ and $C_{TENG} = \frac{8{,}52 \cdot 10^{-15}}{36.76 \cdot 10^{-6} + x(t)}$.

In the simulation, an oscillating DC voltage has been obtained, which reaches peaks of 1.1 V, a value very close to the one measured experimentally (1.071 V).

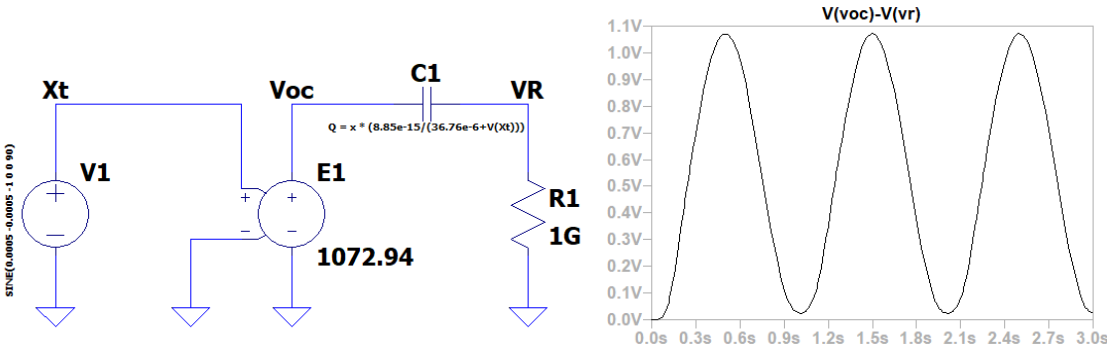

Figure 33: Electric modelling of the manufactured U-TENG and simulation of the voltage obtained.

Moreover, it has been studied the operation in the diode bridge rectifier circuit. The AC voltage obtained from the device has been extracted, together with the DC voltage obtained after the rectifier circuit, with R_{LOAD} of 10MΩ and C_{LOAD} 1μF. For this simulation the output voltage obtained was 7.36 μV negative, and a output current of the order of femtoamperes, i. e. very small electric output (Figure 34A).

The fact that the voltage obtained is so low implies that a bad operation. Therefore, by increasing this voltage, the performance of the system will improve. Among the possible proposals to improve the voltage we find increasing the distance between plates x_{max}, increasing the charge density, which implies increasing the gain of the voltage source dependent on another voltage source, or increasing the frequency of the movement. If we simulate the last case, for a frequency of 25 Hz, we observe that positive rectified voltages are obtained (Figure 34B), but the voltage level is still very low, of the order of microvolts, and insufficient for biomedical applications.

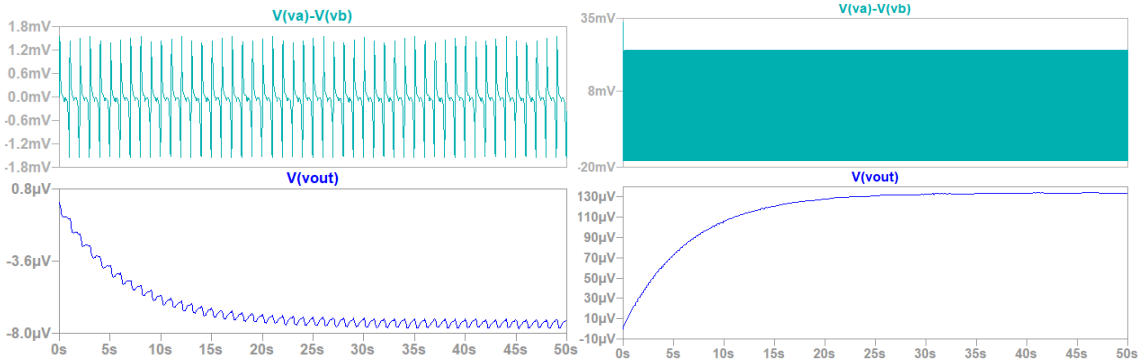

Figure 34: Electric modelling of the manufactured U-TENG and simulation of the voltage obtained.

In addition, measurements have been repeated with the same U-TENG with which 1.071V were obtained, but 4 days later to see if the passage of time meant any alteration or wear of the materials. In this case, the maximum peak measured was 0.529 mV. This may be due to the fact that ITO is a very delicate coating and can be worn, along with the accumulation of dust and others, and this may trigger that the same voltage is not reached.

Another study has taken place in order to observe which is the effect of having an electrode with higher conductivity. The performance of a triboelectric with similar characteristics has been studied, where the electrodes were made of an Aluminium sheet deposited on PET, instead of ITO, as the TENG described in Bhamre et. al. [33] (Bhamre, Mali, & Mane, 2020). With this TENG it has also been observed the triboelectric effect, as a varying DC tension appears when applying mechanical force. However, in this case, the maximum peak voltage values reached were of 699 mV, which is smaller to the one obtained with ITO electrodes.

Furthermore, in Mallineni et. al. [1], it was described that the performance could be improved by adding a cellulose paper sheet between the two plates. However, when introducing the cellulose layer between the plates, it has not been observed any obvious change in the voltage levels.

8 IMPLEMENTATION TIMELINE

8.1 WORK BREAKDOWN STRUCTURE

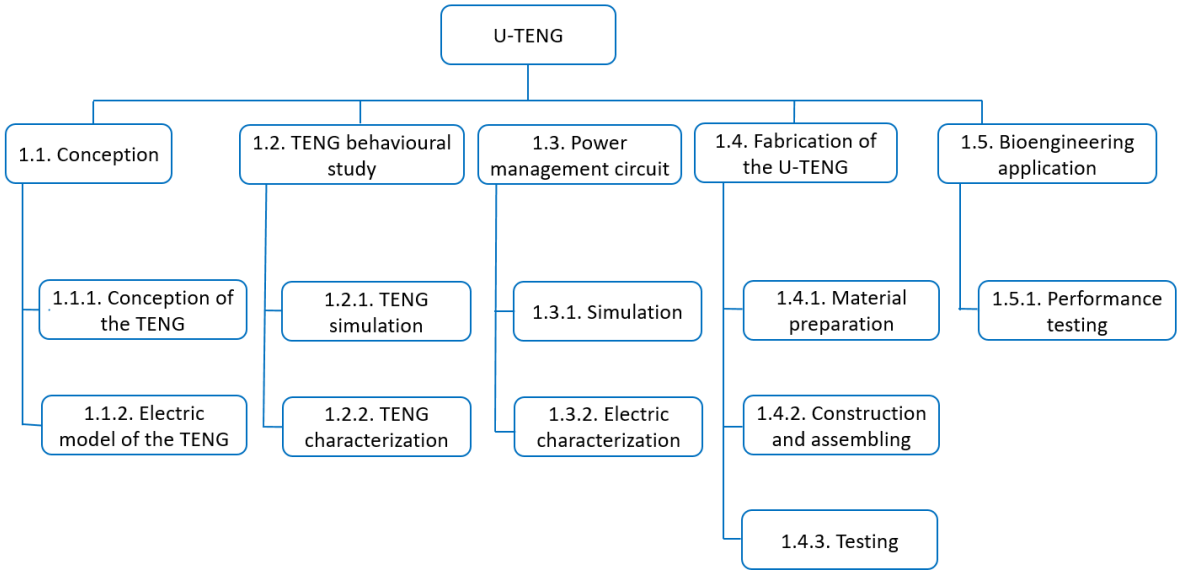

Figure 35: Work Breakdown Structure

8.2 TASK MATRIX AND CPM/PERT

In the following table we define the tasks carried out for the project implementation, indicating an approximation of the time expected to expend, in an optimistic and pessimistic perspective, and the time described in the dictionaries, which is the normal time.

Definition	Task	Precedent tasks	Normal time μ_m	Optimistic time μ_o	Pessimistic time μ_p	Probabilistic time μ_j *
Conception of the TENG	A	-	30	25	35	30
Electric model of the TENG	B	A	10	15	20	13
Material preparation	C	A	5	5	10	6
Construction and assembling	D	C	25	20	35	26
Performance testing	E	D	30	20	40	30
TENG Simulation	F	B	30	25	40	31
TENG electric characterization	G	F	50	40	55	50
Power management circuit simulation	H	G	40	35	45	40
Power management circuit characterization	I	H	60	50	70	60

Performance testing in the bioengineering application	J	E, I	20	20	30	22

Table 9: Task matrix. Time expressed in hours.

The probabilistic time is defined by in the equation 7 and is the one used for the PERT/CPM diagram implementation.

$$\mu j = \frac{\mu o + 4\,\mu m + \mu p}{6}$$

Equation 7: Probabilistic time

The planning involves a total of 14 hours/week, and the date for the beginning of project task execution is programmed to the 9th of November of 2020.

From the data provided in the task matrix, we can develop the PERT/CPM diagram. In this network diagram we define the connectivity between tasks and their dependence on the others, which allows us to find the critical pathways.

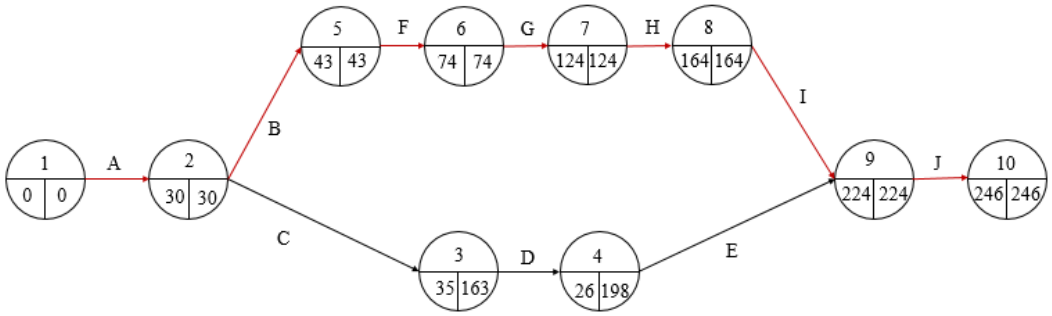

Figure 36: PERT/CPM diagram. In the nodes we observe the early time and last time, in the left and right side, respectively. In red the critical path.

In red we observe the critical path of the project, which may trigger a delay of the project if the tasks included are not carried out on time. This path is the one that determines the duration of the project and on which we must exert more control. We must bear in mind that the times are probabilistic, so that an error on the estimation of the probabilistic time may trigger a change of critical path, as the difference of time with other paths is not very large.

8.3 GANTT TIMING

In order to design the GANTT timing plot, we must define the following table, with the start and final date programmed for each task and their duration.

Description	Task	Start date	Duration	Final date
Conception of the generator	A	09-nov	15	24-nov
Electric model	B	24-nov	5	29-nov
Material preparation	C	29-nov	2.5	01-dec
Construction and assembling	D	01-mar	12.5	13-mar
Performance testing	E	13-mar	15	28-mar

Electric characterization	F	28-mar	15	12-apr
Simulation	G	12-apr	25	07-may
Emulation	H	15-feb	20	07-mar
Integration electronics design	I	07-mar	30	06-apr
Performance testing in the bioengineering application	J	06-apr	10	16-apr

Table 10: Tasks required for the realization of our project with the starting dates and final dates for each. Duration is expressed in days (14 hours/week).

From this schedule we can have an overview of the programmed tasks in a visual way. As the responsible of the development of each task is the same, the performance of tasks simultaneously may trigger an increase of the time per week.

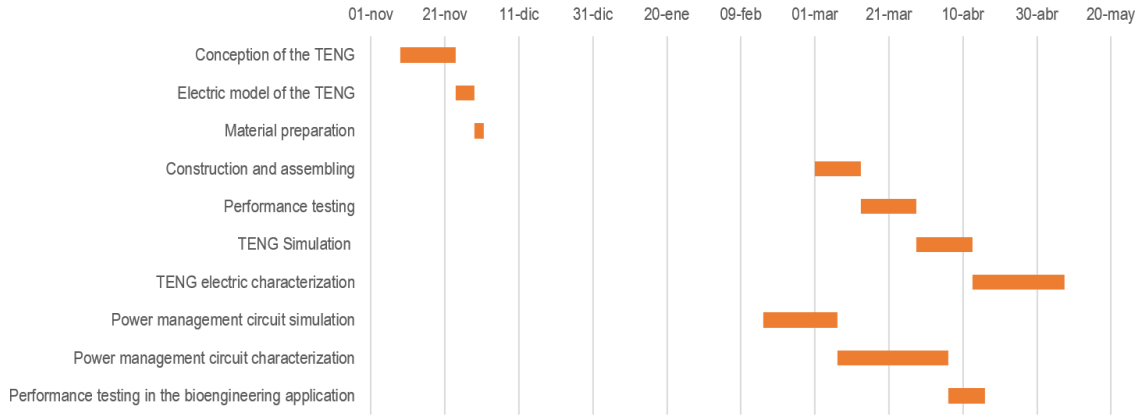

Figure 37: GANTT diagram

9 TECHNICAL FEASIBILITY

For the proposed solution, an analysis has been carried out to study the situation of the project, by making a SWOT matrix of the internal and external characteristics.

	TABLE 11: SWOT MATRIX	
	INTERNAL ANALYSIS	EXTERNAL ANALYSIS
POSITIVE	STRENGTHS - Simple structure, easy manufacturing - Wide range of materials - Inexpensive materials and manufacturing process. - Temperature stability of U-TENG - High output values - Renewable energy from any mechanic motion. - Abundance of starting materials - Robustness - Wide range of load resistances	OPPORTUNITIES - Market trends looking for new forms of sustainable energy. - Development of new biosensors looking for self-feeding systems. - Appearance of new materials and nano-patterning. - Development of structures on stack. - Low commercial prices of the material needed
NEGATIVE	WEAKNESSES - Low current, not directly applicable to active implantable electronic medical devices. - Irregular energy generation for biomedical applications.	THREATS - Limited time - Limited resources - Lack of experience in handling with this technology - Alternative ways of energy harvesting - Mechanical properties may be altered when encapsulating.

Table 11: SWOT matrix of the project

If we refer to the specifications and technical characteristics of the U-TENG, the main advantages are the wide range of materials that can be used, as well as its robustness. Moreover, as we have already indicated above, its manufacture is simple, and the necessary materials are inexpensive. It is a renewable green energy that can be obtained from any form of mechanical energy.

Another strength is that U-TENGs can be used for multiple applications involving different load resistance conditions and can be well rectified. Furthermore, it has been shown in the modelling section that the high output values obtained, both in power and in voltage.

Despite this, for a high output voltage, we obtain a low current, which triggers that the triboelectric generator is not directly applicable to active implantable electronic medical devices. Moreover, although the triboelectric effect has been observed, these high voltages have not been obtained experimentally.

One of the main threats to the viability of this project in biomedical applications is that encapsulation may be necessary to integrate the triboelectric generator into a biocompatible implantable medical device, which may make more difficult to apply an external mechanical force. Another outcome for its applications

in bioengineering is that the energy generation will not be regular, as it depends on a human body motion, which can be altered physiologically.

Among the factors that we can take advantage of to achieve the successful integration of triboelectric generators in the market, we highlight that many lines of research are emerging looking for forms of green and renewable energy. In addition, the design of biosensors by biomedical companies that require a self-feeding system will favour implantation of triboelectric generators. However, it is worth mentioning that alternative products for energy harvesting are also being developed, such as biofuel cells or piezoelectric generators, which may result competitive in the market.

Finally, with the appearance of micro/nano-patterning or similar technologies, the performance of the triboelectric generator can be enhanced by increasing contact area. Furthermore, triboelectric generators can also improve their efficiency by making use of configurations of TENGs on stack.

If we refer to the technical feasibility of the application of the TENG devices manufactured as energy sources for medical devices, specifically for heartbeat harvesting as is the one that has been studied, we can affirm that the constructed triboelectric generators do not provide optimum values for this use. This is why, improvements will be needed at the manufacturing level: such as increasing the effective surface or stacked structures.

10 ECONOMIC FEASIBILITY

As previously mentioned, triboelectric generators in bioengineering applications are in development phase, with the aim of improving their properties and performance, and thus increasing the energy obtained, and consequently the income.

Since the main costs are due to the materials and construction of the structure, it is an inexpensive project. As commercially available materials have been used, obtaining them is much easier and less expensive than if we had to design specific materials from micro/nano-patterning. In addition, the price of the necessary material is low, and few quantities of material are needed, since the designed triboelectric generator has reduced dimensions.

Apart from the price of the materials, we must take into account the cost of assembling the structure. This process is simple and requires little time, since the moulding of the pieces and their handling is simple. Therefore, the cost per hour of labour is not expensive either.

In the article followed for the fabrication [1] (Mallineni et al., 2017), it indicates that the U-TENG can be manufactured with a price of ~ \$0.06 cm^{-2}. Taking basis on the dimensions defined in the article, the budget of the material cost of a single U-TENG has been estimated. It is worth mentioning that the prices that appear in the following table, are approximations obtained from web pages of commercial products. Among the supplying companies and providers, we find Twdrer, Sigma-Aldrich, Katigan and others, all of them distributed by Amazon.

	Commercial price	*One U-TENG cost (€)*
ITO-Coated PET Film	0.01 – 0.05 €/cm^2	~ 0.3
Kapton adhesive tape	0.001 – 0.0006 €/cm^2	~ 0.01
Pyrex insulating spacers	0.01 -0.05 €/cm^2	~ 0.04
Cellulose paper	0.001-0.002 €/cm^2	~ 0.01
Cu wires	0.01-0.004 €/cm	~ 0.04
TOTAL		~ 0.40

Table 12: Cost of fabrication material and process of a U-TENG. Commercial prices obtained from firms and brands that sell their products in Spain. The cost of a U-TENG is calculated by considering the dimensions of 3.5 cm×2.75 cm, two Cu wires of 4 cm, four Pyrex spacers of 4mmx4mm.

However, for this project it has been necessary to manufacture different U-TENGs, in order to test different manufacturing methods, different sizes and others. That is why much more material has been required and the total price of the materials required for the project amounts to a total of 78.66 euros.

	Price	*Brand*
ITO-Coated PET Film	19.96 € (x2)*	Adafruit
Kapton adhesive tape	9.29 €	Changrongsheng
Pyrex insulating spacers	12.9 €	Twdrer
Cu wires	5.05 €	Katigan
Shipping costs	11.5 €	
TOTAL		78.66 €

Table 13: Materials cost. (*) Two ITO-Coated PET Films have been acquired. All the materials have been bought on Amazon.

As a group, and as a student, we have the products under the license from National Instruments, from which we can access different resources and software. For the electrical simulation, LTSpice is a freely available platform.

The university investigation group already has access to the laboratory instrumentation necessary and, therefore, the cost to the project does not depend on its total purchase price, but rather on the amortization of the equipment with respect to the time it will be used. The principal materials used are a digital multimetre for the electric measurements and a laptop. Moreover, as a group, we have access to the products under the license from National Instruments, from which we can access different resources and software. For the electrical simulation, LTSpice is a freely available platform.

If we compare them with other more efficient triboelectric generators, many of them require techniques for micro-structuring the surface or functionalizing it, which increases the cost and manufacturing time. Purchasing commercially available materials reduces the price of our triboelectric generator dramatically. The cost of manufacturing the U-TENG is simply reduced by the low price of the materials that compose it, since its manufacturing does not require any specific type of instrumentation.

The different circuits or power management configurations can also make the final cost of the product vary, depending on its complexity.

11 CONCLUSIONS AND FUTURE LINES

Throughout this research triboelectric generators have been studied as energy harvesters, their modelling, characterization and the design of power management circuits and other strategies that seek to optimize the energy obtained. In addition, their compatibility and possible application in biomedical implants has been studied, considering the size restrictions and characteristics to which they must be adapted. In order to assess the degree of satisfaction with the study carried out, we proceed to discuss the particular objectives that have been met and their degree of achievement.

In the first place, it was proposed to make an electrical model of the triboelectric generator and study different accommodation circuits for our generator. As regards the modelling section, the physics of the TENG has been discussed so that the electric model was consistent with its structure and operation, so that it has been compared to a voltage source and a capacitor that depend on a displacement, modelled as another voltage source. For this simulation, a maximum open circuit voltage of 1.8 kV and a maximum output power peak of 2.92 mW have been obtained, given the material parameters of Table 2. Moreover, the dependence on the different parameters and properties of the materials have been discussed. In the simulation analysis, it has been observed that TENGs behave as a high voltage source, but since the intensity levels are on the order of microamperes, its output power is reduced to milliwatts. Therefore, the objective of simulating an electric model of the triboelectric generator and reproducing the results obtained in other studies has been fully accomplished.

Furthermore, it has been possible to create an accommodation circuit based on a rectifier bridge that allows obtaining a rectified DC signal from an AC. Despite the fact that the DC signal obtained presents good electric output values, with little ripple, the efficiency of this system is very low. Given the time limitation of this project, it has not been possible to study more efficient power management circuits that have a more optimal performance. However, it has been demonstrated through simulations that stack configurations are a valid solution for enhancing electric output power. With the mentioned studies, it has been possible to study the performance of a specific accommodation circuit, its optimum components values and its output electric values. Although we have not been to find more efficient accommodation circuits and compare their performance, as expected in the particular objectives, an alternative method has been proposed to increase the obtained power.

Another of the main objectives of the project was to manufacture a triboelectric generator. Specifically, in this project an attempt has been made to reproduce the U-TENG described in Mallineni et. al. [1] (Mallineni et al., 2017). However, despite the fact that the triboelectric effect has been observed when applying a force periodically, the output values have been much lower than those described in the article. Even so, it has been possible to obtain an open circuit voltage of the order of volts, and the dependence of this output voltage on the surface area has been demonstrated, which was another of the purposes of the project. The differences between the simulation and the results obtained experimentally have been attributed to the manufacturing process and the properties of the materials.

In the particular objectives, it was also expected to make the electric characterization of the manufactured TENG, however, this study has been limited by the low and unsteady values obtained, and unsatisfactory results have been obtained. During the study of the U-TENG performance some worth-mentioning points have been observed. First of all, the signal obtained is considerably unstable. This may be caused by many factors, such as the kind of movement and contact that the plates make. Another fact to bear in mind is that the ITO coating can be easily lost by scratching. Taking into account that our TENG bases its operation on friction and contact, this can lead to the loss of the conductive layer.

Finally, the last objective was to demonstrate the application of triboelectric nanogenerators as self-feeding systems in bioengineering applications. Due to the fact that the electric output of the manufactured TENG, it has not been possible to deepen in their use as self-feeding devices. Therefore, a contingency plan has been applied and a bibliographic study has been carried out on the possible application of triboelectric generators in bioengineering, and specifically for self-feeding implantable medical devices. In it, it has been shown that the use of triboelectric generators is an energy harvesting strategy that meets the supply requirements of the main implantable devices, in addition to presenting a wide range of materials that can be used, many of them biocompatible, and low cost.

11.1 Future lines of the project

The field of energy harvesting is, therefore, a booming area of special interest to the biomedical sector. That is why there is still much to advance and study in this environment, and specifically, for triboelectric generators, which have proven to be a promising strategy.

Regarding the future prospects of this project, different lines of work can be defined. The first one refers to the optimization of the manufactured device. This includes reproducing improvements described in other articles to improve the electrical output of the system [11, 16, 17] (C. Wu et al., 2019)(Kim et al., 2020)(Lee et al., 2017), such as functionalizing or micro-structuring surfaces, or even looking to design new ones. A first approach could be to make use of soft lithography for micro-patterning of the surface, since it is a relatively simple and cheap solution.

To deepen in the study, it would be advisable to develop different triboelectric generators with different pairs of materials and characterize them and compare their performance. Moreover, it is strongly recommended that when testing the performance of the manufactured TENG, a pushing tester is used, so that periodicity is granted, and force modulus and contact area do not vary at each cycle. Another improvement at the modelling and validation study is to deepen in the influence of sigma and surface on the results.

Another line in which progress can be made is in the development of power management circuits, since it has been observed in the modelling and in the experimental part that the TENG gives an AC output that is very irregular, and therefore cannot be directed directly to the electronics of a device as these require a stable DC input. Additionally, the energy harvested that comes from the body environment is quite unstable and can be modified under stress situations.

The energy harvested can be stored in batteries or supercapacitors through power management circuits. However, in this project it has been demonstrated that the efficiency of the system is too low due to the difference in impedance between TENGs and energy storage devices [11](C. Wu et al., 2019). Therefore, it would be interesting to study more advanced rectifying circuits for a better efficiency of energy storage. Two possible approaches are designing power converters for impedance matching or designing a charging cycle to maximize energy transfer [15] (Rodrigues-marinho et al., 2020). In order to stabilize the output voltage, an advanced configuration for a DC-DC circuit could be studied, together with a protection circuit with low consumption.

The study of the application of TENGs in bioengineering applications shows a wide range of options such as comparing the working ranges obtained experimentally with those required by medical devices, studying different biocompatible triboelectric materials or to design a suitable encapsulation to protect the TENG from the body environment but also granting that biomechanical energy is not lost.

Furthermore, the purpose of the introduction of TENGs as power sources is to overcome the limitation of the short lifespan of batteries. However, this hypothesis is based on the idea that TENGs are able to harvest energy without reducing their performance with time. This is why, it would be interesting to carry out a study of the lifetime of TENGs, specifically for liquid-solid friction ones, as they show less abrasion.

Finally, this study has focused on the performance of TENGs as power sources, but it would be desirable to deepen in the performance as active sensors and discuss it sensitivity, stability and its multifunctionality.

12 BIBLIOGRAPHY

1. Mallineni, S. S. K., Behlow, H., Dong, Y., Bhattacharya, S., Rao, A. M., & Podila, R. (2017). Facile and robust triboelectric nanogenerators assembled using off-the-shelf materials. *Nano Energy*, *35*(March), 263–270. https://doi.org/10.1016/j.nanoen.2017.03.043
2. Shi, B., Li, Z., & Fan, Y. (2018). Implantable Energy-Harvesting Devices. *Advanced Materials*, *30*(44), 1–18. https://doi.org/10.1002/adma.201801511
3. Wang, Y., Yang, Y., & Wang, Z. L. (2017). Triboelectric nanogenerators as flexible power sources. *Npj Flexible Electronics*, *1*(1), 1–9. https://doi.org/10.1038/s41528-017-0007-8
4. Wu Z, Cheng T, Wang ZL. (2020) Self-Powered Sensors and Systems Based on Nanogenerators. Sensors. 20(10):2925. https://doi.org/10.3390/s20102925
5. Rao, J., Chen, Z., Zhao, D., Yin, Y., Wang, X., & Yi, F. (2019). Recent progress in self-powered skin sensors. *Sensors (Switzerland)*, *19*(12), 1–19. https://doi.org/10.3390/s19122763
6. Chuan Wu, Chenxing Fan and Guojun Wen. (2019) Self-Powered Speed Sensor for Turbodrills Based on Triboelectric Nanogenerator. https://doi.org/10.3390/s19224889
7. Trung Kien Phan, Song Wang,Yan Wang, He Wang, Xiu Xiao, Xinxiang Pan, Minyi Xu and Jianchun Mi. (2019). A Self-Powered and Low-Pressure Loss Gas Flowmeter Based on Fluid-Elastic Flutter Driven Triboelectric Nanogenerator. https://doi.org/10.3390/s20030729
8. Chen, J., Zhang, C., Xuan, W., Yu, L., Dong, S., Xie, Y., … Luo, J. (2019). Triboelectric nanogenerator-based self-powered resonant sensor for non-destructive defect detection. *Sensors (Switzerland)*, *19*(15). https://doi.org/10.3390/s19153262
9. Chuan Wu, He Huang, Rui Li and Chenxing Fan. (2020). Research on the Potential of Spherical Triboelectric Nanogenerator for Collecting Vibration Energy and Measuring Vibration. https://doi.org/10.3390/s20041063
10. Lee, J. P., Lee, J. W., & Baik, J. M. (2018). The progress of PVDF as a functional material for triboelectric nanogenerators and self-powered sensors. *Micromachines*, *9*(10), 30–33. https://doi.org/10.3390/mi9100532
11. Wu, C., Wang, A. C., Ding, W., Guo, H., & Wang, Z. L. (2019). Triboelectric Nanogenerator: A Foundation of the Energy for the New Era. *Advanced Energy Materials*, *9*(1), 1–25. https://doi.org/10.1002/aenm.201802906
12. Fan, F. R., Tian, Z. Q., & Lin Wang, Z. (2012). Flexible triboelectric generator. *Nano Energy*, *1*(2), 328–334. https://doi.org/10.1016/j.nanoen.2012.01.004
13. Zhong Lin Wang, Jun Chen and Long Lin. (2015). Progress in triboelectric nanogenerators as a new energy technology and self-powered sensors. https://doi.org/10.1039/C5EE01532D
14. Analog devices. LTSpice. https://www.analog.com/en/design-center/design-tools-andcalculators/ltspice-simulator.html
15. Rodrigues-marinho, T., Castro, N., Correia, V., Costa, P., & Lanceros-méndez, S. (2020). Triboelectric energy harvesting response of different polymer-based materials. *Materials*, *13*(21), 1–12. https://doi.org/10.3390/ma13214980
16. Kim, D. W., Lee, J. H., Kim, J. K., & Jeong, U. (2020). Material aspects of triboelectric energy generation and sensors. *NPG Asia Materials*, *12*(1). https://doi.org/10.1038/s41427-019-0176-0
17. Lee, J. H., Yu, I., Hyun, S., Kim, J. K. & Jeong, U. (2017). Remarkable increase in triboelectrification by enhancing the conformable contact and adhesion energy with a film-covered pillar structure. Nano Energy 34, 233–241.
18. Hinchet, R., Ghaffarinejad, A., Lu, Y., Hasani, J. Y., Kim, S. W., & Basset, P. (2018). Understanding and modeling of triboelectric-electret nanogenerator. *Nano Energy*, *47*(January), 401–409. https://doi.org/10.1016/j.nanoen.2018.02.030
19. Niu, S., & Wang, Z. L. (2014). Theoretical systems of triboelectric nanogenerators. *Nano Energy*, *14*, 161–192. https://doi.org/10.1016/j.nanoen.2014.11.034
20. Niu, S., Zhou, Y. S., Wang, S., Liu, Y., Lin, L., Bando, Y., & Wang, Z. L. (2014). Simulation method

for optimizing the performance of an integrated triboelectric nanogenerator energy harvesting system. *Nano Energy*, *8*, 150–156. https://doi.org/10.1016/j.nanoen.2014.05.018

21. Wu, H. T., Wu, H. K., Wang, C. L., Yang, Y. L., Wu, W. H., Tsai, T. H., & Chang, H. H. (2016). Modeling the pulse signal by wave-shape function and analyzing by synchrosqueezing transform. *PLoS ONE*, *11*(6), 1–20. https://doi.org/10.1371/journal.pone.0157135
22. Ouyang, H., Liu, Z., Li, N., Shi, B., Zou, Y., Xie, F., … Li, Z. (2019). Symbiotic cardiac pacemaker. *Nature Communications*, *10*(1), 1–10. https://doi.org/10.1038/s41467-019-09851-1
23. Zheng, Q., Zhang, H., Shi, B., Xue, X., Liu, Z., Jin, Y., … Wang, Z. L. (2016). In Vivo Self-Powered Wireless Cardiac Monitoring via Implantable Triboelectric Nanogenerator. *ACS Nano*, *10*(7), 6510–6518. https://doi.org/10.1021/acsnano.6b02693
24. Santiago Rodriguez, A., Garraud, N., Alabi, D., Garraud, A., & Arnold, D. P. (2019). A simple passive 390 mV ac/dc rectifier for energy harvesting applications. *Journal of Physics: Conference Series*, *1407*(1). https://doi.org/10.1088/1742-6596/1407/1/012018
25. Seol, M. L., Woo, J. H., Jeon, S. B., Kim, D., Park, S. J., Hur, J., & Choi, Y. K. (2015). Vertically stacked thin triboelectric nanogenerator for wind energy harvesting. *Nano Energy*, *14*, 201–208. https://doi.org/10.1016/j.nanoen.2014.11.016
26. Zhao, J., Ghannam, R., Htet, K. O., Liu, Y., Law, M. kay, Roy, V. A. L., … Heidari, H. (2020). Self-Powered Implantable Medical Devices: Photovoltaic Energy Harvesting Review. *Advanced Healthcare Materials*, *9*(17), 1–22. https://doi.org/10.1002/adhm.202000779
27. Cadei, A., Dionisi, A., Sardini, E., & Serpelloni, M. (2014). Kinetic and thermal energy harvesters for implantable medical devices and biomedical autonomous sensors. *Measurement Science and Technology*, *25*(1). https://doi.org/10.1088/0957-0233/25/1/012003
28. Fish RM, Geddes LA. Conduction of electrical current to and through the human body: a review. Eplasty. 2009;9:e44. Published 2009 Oct 12.
29. Zheng, Q., Shi, B., Li, Z., & Wang, Z. L. (2017). Recent Progress on Piezoelectric and Triboelectric Energy Harvesters in Biomedical Systems. *Advanced Science*, *4*(7), 1–23. https://doi.org/10.1002/advs.201700029
30. Wen, DL., Sun, DH., Huang, P. et al. Recent progress in silk fibroin-based flexible electronics. (2021). Microsyst Nanoeng 7, 35. https://doi.org/10.1038/s41378-021-00261-2
31. Zheng Qiang, Bojing Shi, Fengru Fan, et. al. (2014). In Vivo Powering of Pacemaker by Breathing-Driven Implanted Triboelectric Nanogenerator. Advanced Materials 26(33). DOI:10.1002/adma.201402064
32. Ye Ma et. al. Nano Lett. (2016). Self-Powered, One-Stop, and Multifunctional Implantable Triboelectric Active Sensor for RealTime Biomedical Monitoring. 16, 10, 6042–6051. https://doi.org/10.1021/acs.nanolett.6b01968
33. Bhamre, S., Mali, S., & Mane, C. (2020). Optimization of electric vehicle based on triboelectric nanogenerator. *E3S Web of Conferences*, *170*, 3–6. https://doi.org/10.1051/e3sconf/202017001027